



Thalamocortical dynamics of the McCollough effect: boundary-surface alignment through perceptual learning

Stephen Grossberg ^{*,1}, Seungwoo Hwang ², Ennio Mingolla ³

Department of Cognitive and Neural Systems, Center for Adaptive Systems, Boston University, 677 Beacon Street, Boston, MA 02215, USA

Received 4 May 2001; received in revised form 19 February 2002

Abstract

This article further develops the FACADE neural model of 3-D vision and figure-ground perception to quantitatively explain properties of the McCollough effect (ME). The model proposes that many ME data result from visual system mechanisms whose primary function is to adaptively align, through learning, boundary and surface representations that are positionally shifted due to the process of binocular fusion. For example, binocular boundary representations are shifted by binocular fusion relative to monocular surface representations, yet the boundaries must become positionally aligned with the surfaces to control binocular surface capture and filling-in. The model also includes perceptual reset mechanisms that use habituating transmitters in opponent processing circuits. Thus the model shows how ME data may arise from a combination of mechanisms that have a clear functional role in biological vision. Simulation results with a single set of parameters quantitatively fit data from 13 experiments that probe the nature of achromatic/chromatic and monocular/binocular interactions during induction of the ME. The model proposes how perceptual learning, opponent processing, and habituation at both monocular and binocular surface representations are involved, including early thalamocortical sites. In particular, it explains the anomalous ME utilizing these multiple processing sites. Alternative models of the ME are also summarized and compared with the present model. © 2002 Published by Elsevier Science Ltd.

Keywords: Color perception; Binocular vision; Perceptual learning; Visual cortex; Aftereffects; Boundary segmentation; Surface representation; McCollough effect; FACADE model

1. Introduction

A neural model of binocular boundary and surface perception is developed whose adaptive mechanisms can explain a number of key properties of the McCollough effect (ME), including interocular properties which have not previously been explained. The ME (McCollough,

1965) is a complementary color aftereffect, which is typically induced by several minutes of adaptation to gratings of black and color stripes. The ME has many properties that distinguish it from ordinary negative afterimages, including: (1) the ME does not require fixation of adapting stimuli; (2) the ME is orientation-contingent; and, most importantly, (3) the ME can last for hours, days, or even weeks. The ME has attracted much attention because it probes interacting properties of orientational coding, color perception, surface formation, and learning by visual cortex.

McCollough (1965) reported that the ME was monocular; that is, adaptation of only one eye resulted in an effect in the adapted eye but not in the unadapted eye. The absence of interocular transfer of the ME may seem to suggest that binocular loci are not involved in the ME. However, this view has been challenged by subsequent studies which have shown that some interocular properties of the ME do exist, although interocular transfer of the ME does not occur under monocular adaptation.

^{*} Corresponding author. Tel.: +1-617-353-7858; fax: +1-617-353-7755.

E-mail address: steve@cns.bu.edu (S. Grossberg).

¹ Supported in part by the Air Force Office of Scientific Research (F49620-01-1-0397), the Defense Advanced Research Projects Agency and the Office of Naval Research (ONR N00014-95-1-0409), and the Office of Naval Research (ONR N00014-95-1-0657 and ONR N00014-01-1-0624).

² Supported in part by the Defense Advanced Research Projects Agency and the Office of Naval Research (ONR N00014-95-1-0409) and the Office of Naval Research (ONR N00014-92-J-1309 and ONR N00014-95-1-0657).

³ Supported in part by the Defense Advanced Research Projects Agency and the Office of Naval Research (ONR N00014-95-1-0409), and the Office of Naval Research (ONR N00014-01-1-0624).

For example, MacKay and MacKay (1973) found some transfer of visual information between the two eyes. In their experiment, pure orientational information and pure color information was given to each eye separately, such that one eye was adapted to an achromatic grating and the other eye was adapted to a homogeneous colored field. Although neither of the eyes was given an adapting stimulus containing both orientation and color information, a ME was nevertheless induced. Moreover, different aftereffects were obtained for each eye. Testing the color-adapted eye led to a normal aftereffect (that is, the aftereffect exhibits the *complementary* hue to the adapting colored field presented to the same eye), whereas testing the achromatically adapted eye led to an aftereffect that is often referred to as an anomalous ME (that is, the aftereffect exhibits the *same* hue as the adapting colored field presented to the opposite eye). Therefore, in this experiment, both the orientation and color information transferred interocularly to elicit aftereffects. MacKay and MacKay (1973) speculated that some kind of interocular transfer of orientation and antagonistic color might have taken place.

Vidyasagar (1976) was probably the first to provide direct evidence for the idea that binocular neurons are involved in the ME. By using binocular adapting gratings that were colored oppositely to monocular adapting gratings, it was shown that binocular aftereffects can be made opposite to monocular aftereffects.

The interocular properties of the ME were further explored in experiments of White, Petry, Riggs, and Miller (1978), where one eye was adapted to a colored grating and the other eye was adapted to a homogeneous colored field. In those experiments, interocular transfer of orientational information occurred when the color of the homogeneous field was made the same as the color of the grating, but not when the color of the homogeneous field was made the opposite to the color of the grating.

There also have been several attempts to provide theoretical explanations of the ME. Several researchers (Bedford, 1993, 1995; Dodwell & Humphrey, 1990; Shute, 1979; Warren, 1985) have proposed that the ME arises from a process of correcting errors and biases that are imposed during adaptations in ME experiments. Several researchers (Broerse, Vladusich, & O'Shea, 1999; Held, 1980; Hohmann & von der Malsburg, 1978) proposed that the ME arises from neural mechanisms that compensates for chromatic aberration of the eye. For some researchers (Murch, 1976; Allan & Siegel, 1997), common features between the ME and Pavlovian conditioning paradigm were viewed as important characteristics of the ME. Still other researchers focused on how the adaptive mechanisms in the nervous system generate relevant changes in neural loci that subserve the ME as their perceptual outcome. Since the ME is

contingent on orientation, many researchers have suggested that its locus is in the early stages of cortical processing. See Watanabe, Zimmerman, and Cavanagh (1992) for a short review on such neural loci. Some of them suggested that the effect arises from fatigue of neurons that are tuned both to orientation and color (McCullough, 1965; Michael, 1978). Others suggested that the effect arises from synaptic changes in the connection between neurons for orientation and neurons for color (McLoughlin, 1995; Murch & Hirsch, 1972; Savoy, 1984).

In the aforementioned theoretical studies, however, interocular properties of the ME have rarely been emphasized, with the exception of studies by Savoy (1984) and McLoughlin (1995). Savoy (1984) is probably the first to propose a model of the ME that is aimed at explaining interocular properties of the ME. In his model, the ME is generated by an interaction between an orientation system and a color system. Interocular properties of the ME were achieved by positing that the orientation system is binocular and the color system is monocular. However, since the color system in the model is strictly monocular, the model was not able to explain the anomalous ME data of MacKay and MacKay (1973), where there was an interocular transfer of color information.

Recently, McLoughlin (1995) reported data from a wide range of experimental variations regarding interocular properties of the ME, and replicated the experiments of MacKay and MacKay (1973), Vidyasagar (1976), and White et al. (1978), among others. Relative strengths of aftereffects in each experiment were measured in order to collect quantitative data. Then, a neural network model, which resembled the Savoy (1984) model in its overall architecture, was proposed that quantitatively simulated most of these data. Although the model showed a good fit to most of the data, which is remarkable considering its relatively simple architecture, it also exhibited some shortcomings. A major shortcoming is that it did no spatial processing and had no representation of visible surface color. Because it has no processing stage where binocular surface color is represented, it could not explain interocular ME properties, such as the anomalous ME data of MacKay and MacKay (1973). Also, the model implemented orientation-color interactions as an additive operation, rather than as a multiplicative modulation. This hypothesis implies that orientation information, by itself, can lead to an aftereffect in the absence of retinal input to an eye. This property led to some small (around 5% of binocular aftereffect strength), spurious aftereffects when an unadapted eye is monocularly tested, while experimental data suggest that the ME does not transfer interocularly under monocular adaptation.

The present article attempts to overcome these problems and presents a model of binocular vision that

is capable of explaining and quantitatively simulating all the known key properties of the ME, including the interocular properties. The model further develops a neural network theory of binocular vision called FACADE theory (Grossberg, 1987, 1994, 1997; Grossberg & McLoughlin, 1997). Indeed, the first article on FACADE theory (Grossberg, 1987) qualitatively explained a number of ME data, including interocular properties, but did no simulations to quantitatively test its validity. A key hypothesis of the Grossberg (1987) model is further developed herein; namely, that the ME arises using visual system mechanisms whose primary functions are to adaptively align boundary and surface representations which are positionally shifted with respect to one another due to the process of binocular fusion and allelotropia, or displacement (Rose, Blake, & Halpern, 1989; von Tschermak-Seysenegg, 1952; Werner, 1937), in the boundary system, but not in the surface system, of the visual cortex (Grossberg, 1987). Thus the Grossberg (1987) proposal replaces an orientation and color system by a boundary and surface system. The properties of these boundary and surface systems have elsewhere been used to explain many other types of perceptual and neurobiological data. Since boundaries are used to form the compartments which surface brightness and color signals fill-in, the signals between the boundary and surface systems must be positionally aligned. The FACADE model predicts that the signals between the boundary system and the surface system undergo perceptual learning in order to compensate for their mutual displacement. The model also proposes that such adaptive alignment mechanisms are activated by habituated transmitter gates in chromatic opponent processing circuits. These additional mechanisms assure that percepts are rapidly reset in response to temporally changing scenes (Francis & Grossberg, 1996; Francis, Grossberg, & Mingolla, 1994). The present article shows how to rigorously incorporate such perceptual learning and habituated mechanisms into FACADE theory. The ME is then induced as an emergent phenomenon of these adaptive alignment and habituated mechanisms. The model's proposal of how this happens provides a functionally meaningful explanation of the ME data as a manifestation of boundary and surface interactions. The present article shows how a quantitative implementation of these FACADE mechanisms, which have not been implemented together before, can quantitatively simulate all the key data.

2. Theory

2.1. Overview of FACADE theory

FACADE theory suggests that the brain's representation of a visual scene is generated by interactions

between two main subsystems: the Boundary Contour System (BCS), and the Feature Contour System (FCS). The BCS forms binocular boundary segmentations that do not carry any visible signal; they are invisible or amodal. The FCS fills in visible surface properties at spatial locations whose boundaries are determined by the BCS. The BCS models properties of the interblob cortical stream, and the FCS models properties of the blob cortical stream (Grossberg, 1994).

Previous works on FACADE theory have shown how it can explain a variety of perceptual and neural data about 3-D vision and figure-ground perception (Grossberg, 1987, 1994, 1997; Grossberg & Kelly, 1999; Grossberg & McLoughlin, 1997; Grossberg & Pessoa, 1998; Kelly & Grossberg, 2000). In the present article, FACADE theory is further developed in order to quantitatively model the processing stages that are needed to explain ME data. For simplicity, details of FACADE theory that are not needed for this aim are omitted.

A key property of 3-D vision, and of FACADE's explanations thereof, drives our present model development. Fig. 1(a) illustrates this property, which is

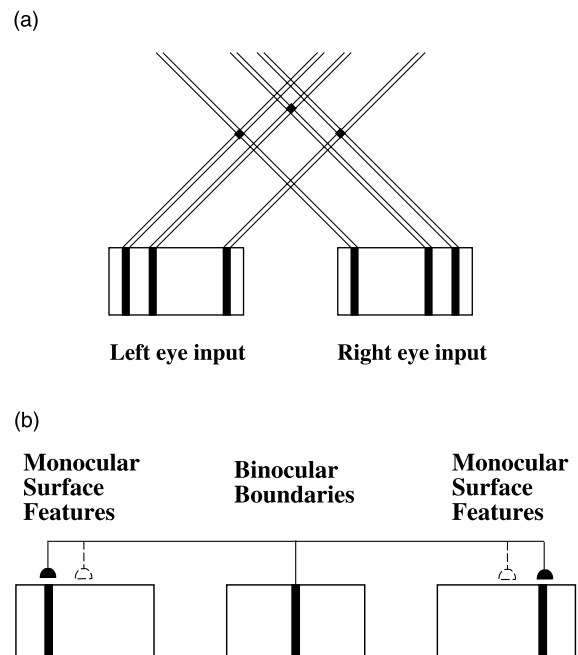


Fig. 1. Illustration of allelotropia. (a) Stimulus is composed of three bars. The two outermost bars fall onto corresponding retinal points, whereas left and right eye positions of the middle bar are disparate. Yet when fused, the middle bar is seen at a midpoint between the two disparate monocular positions. (b) The brain needs to map between the binocular boundary position of the fused middle bar and the disparate surface positions of the two monocular middle bars. This mapping is proposed to occur through learning based on their mutual correlation during visual development. Filled and open hemispheres denote adaptive synapses learned from strong and weak positional correlation, respectively.

classically called allelotropia, or displacement (Rose et al., 1989; von Tschermak-Seysenegg, 1952) and is due to the basic fact that left and right eye images of an object in depth are registered at disparate spatial locations on their respective retinas. Fig. 1(a) shows a display in which three bars are presented to the left and right eyes. The outermost bars are in register, but the middle bars are not. The figure also shows that the left and right eye images of the middle bar are displaced to form a fused binocular image at a location midway between each monocular bar. The same phenomenon occurs, say, when viewing the letters ABC and A BC with the left and right eyes, respectively. Then B is seen in the middle of the display at a different depth than A and C.

In FACADE theory, the boundaries that are formed from information about both eyes are used to control which surface representations fill-in their perceived surface brightnesses and colors. When a scene is viewed with both eyes, fused binocular boundaries are shifted relative to their corresponding monocular representations of surface features. Different amounts of shift are, moreover, caused at different relative depths from the observer. The brain needs to align these boundaries and surface features in order to control the surface filling-in process. FACADE theory predicted (Grossberg, 1987) that alignment is carried out by a learning process which adaptively links the corresponding boundary and

surface signals, as illustrated in Fig. 1(b). The present article illustrates how this functionally meaningful hypothesis can quantitatively simulate ME data when it is mathematically embodied within the FACADE framework. In particular, the adaptive alignment of boundaries and surfaces at several monocular and binocular processing stages, when combined with habituated and opponent circuits that dynamically reset perceptual representations in response to changing imagery, are sufficient to simulate all the main properties of the ME.

2.2. Overview of the present model

Fig. 2 provides an overview of the FACADE model that is developed in the present article. The processing stages in the model are next described before their functional roles in explaining the ME are summarized.

The first model stage (Fig. 2, Stage I) consists of three sets of retinal or lateral geniculate nucleus (LGN) cells that are activated by the stimulus distribution in each eye. This stage is modeled as simply as possible to include only the properties that are needed to explain the targeted data. One set of cells (denoted as A in Fig. 2) is activated mostly by achromatic stimuli. The other two sets of cells (denoted as M and G in Fig. 2) are activated mostly by magenta or green stimuli, respectively. Cells

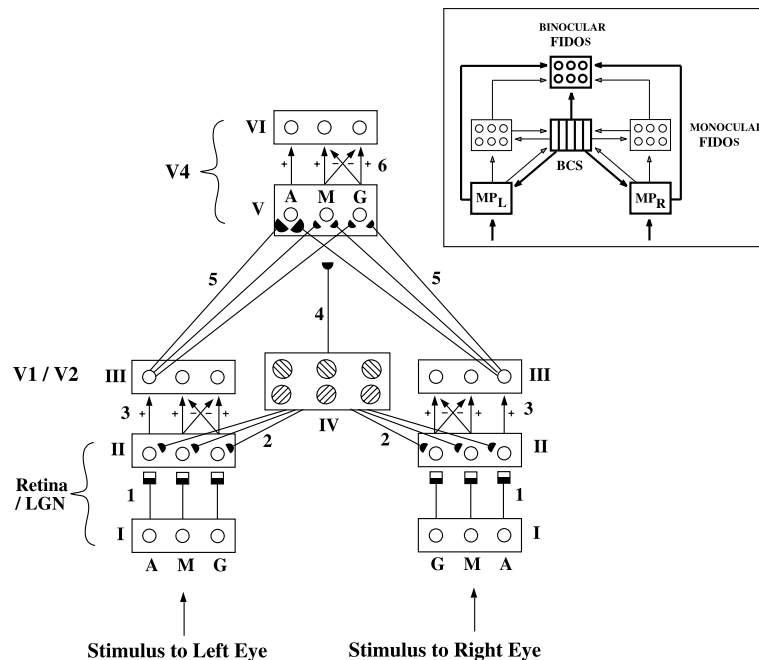


Fig. 2. Schematic diagram of the FACADE model used to simulate ME data. Hatched circles denote BCS cells that are tuned to orientation (45° and 135°) and to ocularity (left monocular, binocular, and right monocular). Three pairs of open circles denote FCS cells tuned to three colors (achromatic (A), magenta (M), and green (G)). Processing stages in the theory are numbered by Roman numerals. Pathways that connect those processing stages are numbered by Arabic numerals. Pathways that end with hemicircles are gated by adaptive synaptic weights. Pathways that end in black and white squares are gated by habituated or depressing synapses. Pathways that end in arrowheads merely transfer signals from one cell to another. The inset shows a macrocircuit of the FACADE model, including stages and pathways that were implemented in this study (drawn by bold lines), as well as those were not (drawn by thin lines), which are employed in explanations of other phenomena. See text for details.

are modeled using feedforward networks with circular concentric on-center off-surround receptive fields that input to cells which obey membrane, or shunting, equations. The properties of these cells, such as discounting the illuminant, contrast normalization, and sensitivity to image reflectances, were discussed in detail by Grossberg (1973, 1983) and used to explain various brightness perception data by Grossberg and Todorović (1988).

Output signals from LGN cells are multiplied, or gated, by habituating or depressing transmitters (Grossberg, 1968, 1969); see Fig. 2 (Pathway 1, square synapses). The transmitter habituation is proportional to the strength of the input signal and to the amount of available transmitter. Our model of transmitter habituation is consistent with Abbott, Varela, Sen, and Nelson (1997)'s experimental and modeling work on synaptic depression in cortical cells. Such transmitters play a key role in achieving intracellular adaptation (Carpenter & Grossberg, 1981); rebalancing and resetting neural circuits (Baloch, Grossberg, Mingolla, & Nogueira, 1999; Francis & Grossberg, 1996; Francis et al., 1994) as well as, in suitable parameter ranges, generating transient neural responses (Baloch et al., 1999; Ögmen & Gagné, 1990). They also play a fundamental role in our ME explanations.

The cells in model areas V1 and V2 of the BCS (Fig. 2, Stage IV) become active when oriented boundary structures in the stimulus are detected. The BCS contains binocular cells, left monocular cells, and right monocular cells. In this article, the term “binocular cells” refers to cortical cells that are driven equally well by either of the two eyes, and the term “monocular cells” refers to cortical cells that show a strict ocular dominance. Both types of cells are well known to exist (Hubel & Wiesel, 1962). The model does not need to invoke intermediate cell types to simulate ME data. Previous modeling work (Grossberg & McLoughlin, 1997) showed how both types of cells contribute to stereopsis and 3-D boundary and surface perception. The present model further assumes that the binocular cells behave as “OR” gates that respond strongly to binocular stimuli and weakly to monocular stimuli (Hubel & Wiesel, 1962; Pettigrew, Nikara, & Bishop, 1968). The monocular cells, on the other hand, are assumed to respond strongly to monocular stimuli and weakly to binocular stimuli (Kato, Bishop, & Orban, 1981). The relative strengths of binocular and monocular cells under binocular and monocular stimulus presentations are key parameters in the present simulations.

In most FACADE simulations (e.g., Grossberg & McLoughlin, 1997; Grossberg & Todorović, 1988), activation of BCS cells is usually computed by simple and complex cell stages that directly extract edge information from an image. In the present simulations, however, activation of BCS cells is simplified by assigning a given

value to BCS cells located at the positions corresponding to edges of input stimuli. This was done to simplify our simulations, which focus upon the habituating and learning dynamics of several monocular and binocular processes from LGN through cortical area V4, as in Fig. 2. See Eq. (15) in Appendix A for details on how the BCS cell activities are obtained in the present simulations.

Once activated, these BCS cells send signals along two types of pathways. One of them is a binocular boundary pathway (Fig. 2, Pathway 4). It interacts with binocular featural signals to form a visible surface representation by a mechanism of filling-in, as will be described later. The other is a top-down feedback pathway (Fig. 2, Pathway 2) from model area V1 to LGN. Consistent with the architecture of the present model, Grieve and Sillito (1995) reported that both binocular and monocular cells are found in corticogeniculate projecting neurons in layer 6 of the primary visual cortex in cats. Both modeling (Gove, Grossberg, & Mingolla, 1995; Grossberg, Mingolla, & Ross, 1997) and experimental (Sillito, Jones, Gerstein, & West, 1994) studies have suggested that the functional role of the corticogeniculate feedback pathway is to select and enhance LGN cell activities that are consistent with cortical cell activities. Other modeling studies (Grossberg, 1980; Grunewald & Grossberg, 1998) further predicted that this feedback pathway possesses adaptive synapses and showed how these adaptive synapses in the feedback pathway undergo experience-dependent learning which helps to stabilize the tuning of binocular disparity in feedforward pathways. A recent study by Murphy, Duckett, and Sillito (1999) showing that these feedback signals to the LGN are spatially distributed with the same orientation as their cortical sources is consistent with the prediction that their synapses can learn.

In addition to these previously suggested functions of the corticogeniculate feedback pathway, the present article proposes how this feedback pathway can also contribute to the ME. This is predicted to occur through modification of its adaptive synapses in response to transmitter habituation in LGN cells that is induced by prolonged viewing of adapting gratings. The learning in the model corticogeniculate feedback pathway tracks postsynaptic cell activity and is gated by the correlated activities of its presynaptic and postsynaptic cells. As a result, the strength of the pathway changes only when V1 (presynaptic) cells and LGN (postsynaptic) cells are concurrently active. In this manner, the corticogeniculate feedback pathway learns the transmitter-gated LGN cell activities with which the V1 cells are associated. The theory hereby proposes that the effects of this process on the ME are due to the combined effects of the habituation-reset properties of transmitter gates and the stabilizing properties of top-down learning. It should also be noted that *any* feedback pathway from the

boundary cells to monocular surface representations could play the same role, notably connections from V2 interstripes to thin stripes, which play a key role in FACADE explanations of figure-ground percepts (Grossberg, 1997; Kelly & Grossberg, 2000). It is possible that multiple (binocular boundary)-to-(monocular surface) interactions influence the ME in tandem, but only the LGN path will be simulated, for simplicity.

The corticogeniculate feedback pathway not only learns the transmitter-gated LGN activities, but also influences the LGN signals through multiplicative gating. Thus, oriented boundary activity modulates the activity of LGN cells that already receive retinal input. Several studies have reported neurophysiological data that support such a modulatory interaction; e.g., Przybyszewski, Gaska, Foote, and Pollen (2000) and Sillito et al. (1994).

The multiplicative combination of bottom-up transmitter-gated and top-down learned signals is then further transformed by monocular opponent processing (Fig. 2, Pathway 3) between magenta and green cells to give rise to monocular featural signals (Fig. 2, Stage III). The Stages I–III comprise the monocular FCS. These monocular featural signals are conveyed by the cortical bottom-up FCS pathway (Fig. 2, Pathway 5) to the next stages of surface processing, where the outputs from the monocular FCS are binocularly matched and subsequently filled-in (Fig. 2, Stage V). In the present and previous works on FACADE theory, one function of this pathway was to adaptively align the monocular FCS surface signals with binocular BCS boundaries that are positionally displaced by binocular fusion and allelotropia so that the BCS could control binocular filling-in of 3-D surfaces within the FCS. Grossberg and Kelly (1999) tested the binocular filling-in function by simulating data on binocular brightness perception, including Fechner's Paradox. Here we introduce a learning law into this pathway and show how it can help to explain the ME.

Binocularly summated featural surface properties, such as color, generate a visible surface representation at the final level of the FCS, which is called the binocular Filling-In-Domain (FIDO). The binocular FIDO (Fig. 2, Stages V and VI) includes arrays of intimately connected cells such that neighboring cells can rapidly spread activities between each other's compartment membranes. This diffusive spreading, or filling-in, of activation is initiated by binocularly matched featural inputs and is restricted to the compartments that are formed by binocular boundaries (Fig. 2, Pathway 4), which act as barriers to filling-in. The net effect of these interactions is that the binocularly summated featural surface properties spread within binocular boundaries. The resultant filled-in activities of magenta and green binocular FIDOs are opponently processed (Fig. 2, Pathway 6) to yield a perception of surface color.

Together with the cortical bottom-up FCS pathway, the binocular boundary pathway is used to explain the anomalous ME data of MacKay and MacKay (1973), among others.

2.3. Qualitative model explanation of general ME properties

Core issues in the ME that need to be explained by any theory include why the effect is typically complementary to the adapting color, how the effect becomes long-lasting, and how the effect becomes contingent on orientation. The present theory explains these general properties as follows.

Consider what happens in the network in response to 45° binocular adapting gratings of magenta and black stripes. As shown in Fig. 3, prolonged presentations of the adapting gratings substantially habituate magenta transmitters in the LGN (shown as squares that are filled in by smaller black areas in Pathway 1). This habituation of neurons is the basis of the model's explanation of the ME, as in so-called fatigue models. At this point, a natural question is, how can the long duration of the ME, which is clearly longer than the time scale of transmitter depletion and recovery, be explained?

The model proposes that corticogeniculate feedback pathways (Pathway 2) possess adaptive synapses (shown as hemicircles at the end of Pathway 2) that learn long-term changes in synaptic efficacy. The synaptic strength is hypothesized to track the transmitter-gated signal. Since the transmitter habituates, the net result of these changes is a weakening of the synaptic strength. In this

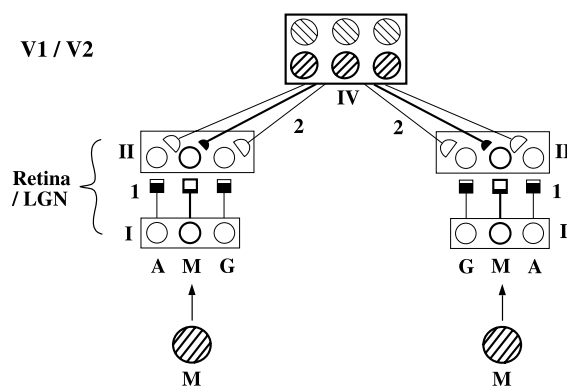


Fig. 3. Schematic diagram of corticogeniculate learning in the model in response to 45° binocular gratings of magenta and black stripes. Cells and pathways that are stimulated by the adapting gratings are drawn in bold lines. Unstimulated cells and pathways are drawn in thin lines. Open hemicircles denote the adaptive synapses that have not learned under current adaptations. Filled hemicircles denote the adaptive synapses that have learned under current adaptations. In order to facilitate the explanation, the illustration is simplified in the following ways: (1) only the relevant stages (up to Stage IV) of the model are depicted; (2) relative strengths of binocular and monocular cortical cells are not depicted. See text for details.

way, a transient magenta transmitter habituation is encoded in the long-term synaptic efficacy in the corticogeniculate feedback pathways that project to magenta LGN cells (shown as smaller filled hemicircles in Pathway 2), while the synaptic efficacy of feedback pathways to green LGN cells remains unchanged (shown as larger open hemicircles in Pathway 2).

On test trials, both the magenta and green retinal cells are equally activated by an achromatic test grating. The synaptic learning caused by prior magenta adaptation, however, causes smaller output signals to be generated from magenta LGN cells than from green LGN cells. Since the output signals from LGN cells are then opponently processed, a net green monocular color signal is generated. When the net green signals from each eye are then binocularly summed and filled-in at the binocular FIDO, a green aftereffect is observed. Since the synaptic change, or learning, is driven by transmitter habituation, which is a cumulative process, the learning is also a cumulative process. This property is consistent with the data of Skowbo and White (1983), who showed that the acquisition of the ME depends on the duration, not on the number, of adapting stimulus presentations. Simulations of the habituating process under a number of presentation conditions (not reported here) have confirmed this property of the model.

How can the orientation sensitivity of the ME be explained? This property of the ME comes from the orientation sensitivity of BCS cells. Since the gratings used in ME experiments involve only two orientations that are mutually perpendicular, the orientation sensitivity of BCS cells is modeled in a simple way, such that each BCS cell responds to one orientation, but not to the other. For example, when a 45° grating is presented, a subpopulation of BCS cells that are tuned to 45° orientation becomes activated while a subpopulation of cells that are tuned to 135° orientation is inactive, and vice versa. Since the synaptic learning in the corticogeniculate feedback pathway is proposed to take place only when V1 (presynaptic) cells and LGN (postsynaptic) cells are concurrently active, the synaptic learning becomes contingent on orientation. An adaptation to a 45° magenta grating, for example, leads to the weakening of synaptic strength along the pathways from 45°-tuned V1 cells to magenta LGN cells, but not along the other pathways. Therefore, a green aftereffect is observed with a 45° test grating, but not with a 135° test grating. Similarly, an adaptation to a 135° green grating elicits a magenta aftereffect only when tested with a 135° test grating, but not with a 45° test grating.

There are three types of adaptive pathways in the model. One is the corticogeniculate feedback pathway, another is the cortical bottom-up FCS pathway, and the third is the binocular boundary pathway. As described above, the general ME properties—namely, how the effect is typically complementary to the adapting color,

and how the effect becomes long-lasting and contingent on orientation—can be explained by using the adaptive mechanisms of the corticogeniculate feedback pathway, or indeed any other early boundary-to-surface pathway with similar properties.

What role, then, do the cortical bottom-up FCS pathway and the binocular boundary pathway play for the ME? We propose that the adaptive mechanisms in these pathways play a critical role in explaining anomalous ME data of MacKay and MacKay (1973) and interocular ME data of White et al. (1978), but not in explaining the general ME properties described above. The reason why the adaptive mechanisms of the cortical bottom-up FCS pathway do not play a critical role in explaining core ME data comes from the fact that, in typical ME experiments, binocular adapting gratings presented to the two eyes are of the same color. In such cases, the colors registered in the monocular and binocular FCS agree with each other. For example, magenta cells in the monocular FCS are normally connected to magenta cells in the binocular FCS. With magenta adapting gratings presented binocularly, magenta cells in the monocular FCS continue to connect to magenta cells in the binocular FCS, and the cortical bottom-up FCS pathway is largely unaltered. The same explanation holds also for monocular adaptations, since the monocular color and the binocular color also agrees with each other in such cases. When the colors presented to the two eyes are different, as in the experiments of MacKay and MacKay (1973) and of White et al. (1978), colors within the monocular and binocular FCS may not agree. This difference helps to explain these data, as detailed later.

3. Quantitative model explanations and computer simulations of multiple ME cases

Thirteen cases of ME experiments from McLoughlin (1995) were simulated in order to examine how closely simulations of the present model match experimental data. Simulations of the model were performed using the equations presented in Appendix A with a single set of numerical parameters. Differential equations of the model were solved either at equilibrium or by numerical integration, as described in Appendix A.

In the experiments of McLoughlin (1995), the adapting and test stimuli subtended 8° of visual angle with stripes at 2 cpd. In the present simulations, the stimuli were represented as one-dimensional luminance distributions of one black and two colored stripes on a black background. This representation was adopted to simplify the simulations. A more realistic representation (e.g., more stripes in the stimuli) is expected to yield similar simulation results because learning in the model is based on the local correlation between neighboring

boundary and habituated color signals within each stripe in the adapting stimuli.

Opponent-processed filled-in activities of binocular FIDO color cells comprised the final outputs from the network. Such filled-in activities observed in response to achromatic test gratings correspond to the color aftereffects observed in the ME experiment; that is, red filled-in binocular FIDO activities at the positions corresponding to the white stripe regions of achromatic test gratings indicate a red aftereffect, and green activities indicate a green aftereffect. The filled-in value corresponding to the middle spatial position in the white stripe regions was compared to the experimental data, which describe the relative strengths of aftereffects. Since the filled-in regions are flat, other measures (such as an average of filled-in values in the white stripe regions) would yield nearly the same value as the filled-in value at the middle spatial position in the white stripe regions.

For each of the 13 cases of ME experiments simulated herein, three phases of simulations were necessary; namely, a weight-initialization phase, an adaptation phase, and a test phase. During the weight-initialization phase, initial values of all synaptic weights are learned. Weight-initialization strives to learn weight values that the system would have learned under normal conditions; that is, prior to ME adaptations. Weights first start out small and equal for all spatial locations in the network, followed by training of the network until a proper topographic mapping between the BCS and the FCS is established. The training stimuli are gratings with the same amplitude and pattern as the gratings used in ME adaptations. For example, 45° magenta gratings are used to train all the pathways that involve cells for 45° orientations and magenta colors. The same is true for the other orientation and the other colors. Weight-initialization learning employs binocular gratings and no transmitter habituation because humans usually view the world binocularly and do not usually stare at objects long enough to cause major amounts of transmitter habituation. In response to the training stimuli, topographic mappings in the three adaptive pathways self-organize according to the correlated activities of their presynaptic and postsynaptic neurons. The values of the self-organized weights are the initial values with which ME adaptation and learning subsequently take place.

During the adaptation phase, adapting stimuli are presented to the network for a prolonged length of time. As a result, the transmitter gate becomes habituated and the weights in the three adaptive pathways change in strength according to the correlated activities of their presynaptic and postsynaptic neurons. Five minutes of adaptation corresponds to 40 iterations of numerical integration. Among the 13 cases of ME experiments, some employ 5 min of adaptation and others employ longer adaptation. In the simulations, it will be seen how longer adaptation, implemented by a larger number of

iterations, leads to more transmitter habituation and learning, resulting in stronger aftereffects. In experiments of McLoughlin (1995), adapting stimuli were alternated at every 5 s. In the present simulations, however, adapting stimuli are presented continuously to the network for simplicity. This simplification is not expected to have a considerable effect on the present simulations because results are expressed as *relative* strengths across multiple experimental cases. If the same presentation paradigm is used consistently for all cases, relative strengths are not expected to be affected. Also, their absolute strengths may not be expected to be substantially affected. As noted in Section 4 of this article, simulations have shown that the duration of stimuli, rather than the number of stimulus presentations, is the dominant factor in determining the course of habituation.

During the test phase, transmitter levels are set to an initial resting level while learned synaptic weights in the three adaptive pathways are maintained at existing levels, on the premise that transmitter dynamics are transient and learned synaptic efficacy is a long-term effect. As a result of prior learning, achromatic test gratings elicit chromatic outputs from the network, whose measure was described earlier. The output measure is then compared to the experimental data. In all 13 experiments and simulations, the following procedures commonly apply: (1) the strengths of aftereffects are obtained using test gratings shown to the left eye only (left monocular test), to the right eye only (right monocular test), and to both eyes (binocular test); and (2) the strength of aftereffect from the binocular test in the standard binocular case, shown in Fig. 4, is used to normalize all other results as a percentage value.

Although there are many parameters in the model, the parameters for the binocular and monocular BCS cell activities under binocular and monocular stimulations (B_B , B_M , M_M , M_B) have been of particular interest because they play a crucial role in governing how strongly corticogeniculate learning occurs during adaptation, and how strongly LGN activities are gated during test. They are also important because the comparison data consist of relative aftereffect strengths across multiple experiments that probe various monocular, binocular, and interocular interactions during the ME induction and test. During the parameter search phase of our research, the relative BCS cell activities determined by these four parameters were varied while all other parameter values were fixed across cases. Thus, they were the key parameters that were explored in the simulations to fit the experimental data. They were chosen in the range between 0 and 1 and obeyed the intuitive and physiological constraints (Hubel & Wiesel, 1962; Kato et al., 1981; Pettigrew et al., 1968) that $B_B > B_M$ (binocular cells are more active under binocular stimulations than monocular stimulations), $M_M > M_B$ (monocular cells are more active under monocular

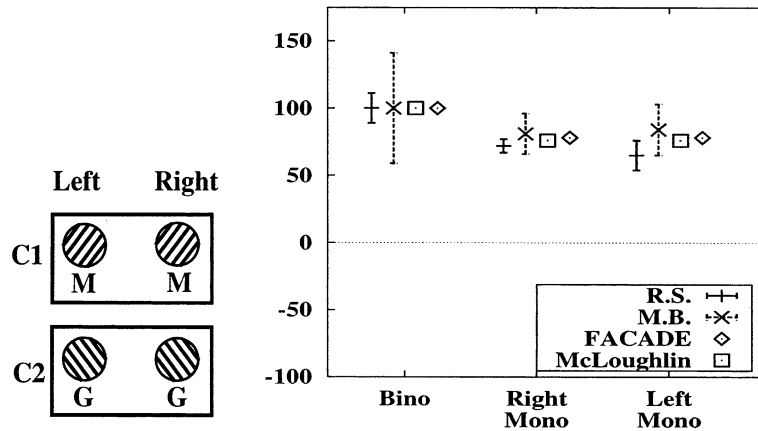


Fig. 4. Standard binocular case: (Left) Adapting stimuli used. (Right) Experimental data and simulation results for the McLoughlin and FACADE models.

stimulations than binocular stimulations), $B_B > M_B$ (binocular cells are more active under binocular stimulations than monocular cells), and $M_M > B_M$ (monocular cells are more active under monocular stimulations than binocular cells).

The first two cases (standard binocular and standard monocular) were simulated first in order to find ranges of these four parameter values that fit them. Within those workable parameter ranges, all the remaining cases were then simulated in order to obtain combinations of parameter values that fit all cases. Qualitative understanding of network dynamics helped this parameter search processes. For example, increasing B_B was expected to yield an increase in aftereffects in cases where binocular adaptations or binocular tests were employed. The reported parameter sets are not, however, necessarily optimal, since we know of no practical method to optimize such a complicated data fit to a hierarchically organized network with multiple spatial and temporal scales.

3.1. Standard binocular case

In the Standard Binocular Case, the two eyes are adapted to the same binocular adapting gratings. A pair of such gratings of opposite color and orientation (that is, 45° magenta gratings and 135° green gratings) is sequentially alternated for 5 min. Thus, each grating is presented for 2.5 minutes. Unless stated otherwise, all experiments simulated in this article use two and one-half minutes as an adaptation time for each grating of a given configuration. Fig. 4 summarizes the adapting stimuli (where C1 and C2 refers to the configuration of each adapting grating), along with a plot showing the experimental data from two subjects (RS and MB) with standard deviations, simulation results from McLoughlin (1995), and simulation results from the present model (FACADE), all under binocular test (Bino), right mon-

ocular test (RightMono), and left monocular test (LeftMono).

The main finding of the Standard Binocular Case is that the aftereffect induced by binocular adaptations is stronger in the binocular test than in the monocular test. This is explained in the present model as follows. During binocular adaptations, synaptic learning takes place in both of the corticogeniculate feedback pathways that project to the left and the right LGN. Upon binocular test, both learned pathways are used, since LGN cells in both eyes are stimulated by binocular test gratings. Therefore, monocular color signals are generated by both eyes. Upon monocular test, on the other hand, only one of the two pathways is used. Thus, monocular color signals are generated only by one eye. By the process of nonlinear binocular brightness summation (Grossberg & Kelly, 1999), the summated binocular color signals become greater in the binocular test than in the monocular test, although such a summation is not linear. When such binocular color signals are subsequently filled-in, the aftereffect becomes greater in the binocular test than in the monocular test, as shown in Fig. 4.

We have also investigated how the strength of the aftereffect is influenced by presenting the same binocular adapting gratings twice as long, as shown in Fig. 5.

By comparing Fig. 5 to 4, it can be seen that the aftereffects become stronger when the adaptation period is made twice as long. This is true in the model because both the transmitter habituations in the LGN and the resultant synaptic changes in the corticogeniculate feedback pathways are cumulative processes that depend on the duration of adapting stimulus presentations.

3.2. Standard monocular case

The Standard Monocular Case shows that monocular adaptations yield an aftereffect in the adapted eye, but

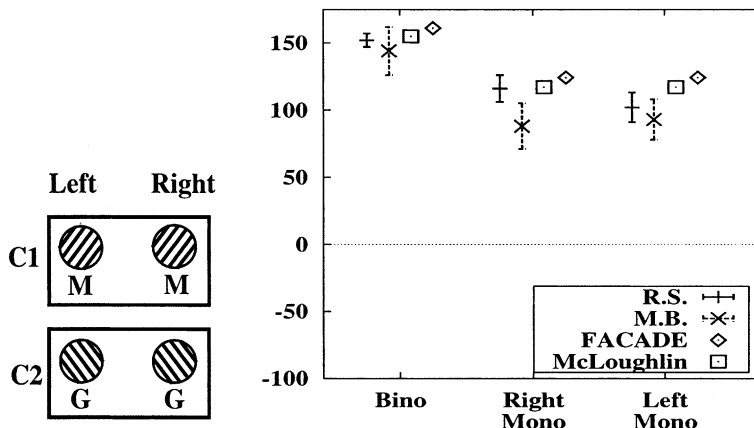


Fig. 5. Standard Binocular Case with longer adaptation: (Left) The same adapting stimuli as in the standard binocular case is used while adaptation period is made twice as long. (Right) Experimental data and simulation results for the McLoughlin and FACADE models.

not in the unadapted eye. Here, only the right eye is adapted to monocular gratings. A pair of such gratings of opposite color and orientation is sequentially alternated. Fig. 6 summarizes the stimuli and results.

As shown in Fig. 6, the aftereffect is confined to the adapted eye only (the right eye). Why does interocular transfer not occur? The absence of interocular transfer is explained by the architecture of the model and the learning law that is used. Fig. 7 shows what happens to the network during monocular adaptations. In particular, synaptic learning occurs in the corticogeniculate feedback pathway only when V1 (presynaptic) cells and LGN (postsynaptic) cells are concurrently active. Since LGN cells in the unadapted left eye are inactive during the right monocular adaptation, no synaptic learning occurs in the corticogeniculate feedback pathway projecting to the left LGN (shown as thin lines that end in open hemicircles in Fig. 7). Also, since the left monocular cortical cell is inactive during the right monocular adaptation, no synaptic learning occurs in the cortico-

geniculate feedback pathway projecting from the left monocular cell (shown as an absence of the left monocular cell and of its feedback pathway). Thus, the aftereffect is not observed in the unadapted left eye, and therefore does not transfer interocularly.

How, then, does the binocular test yield a weaker aftereffect than does the right monocular test? This weaker binocular aftereffect comes from the property that binocular cells are less active than monocular cells under monocular stimulations (shown as smaller “B” compared to larger “R” in Fig. 7). Since synaptic learning is gated by activities of both V1 (presynaptic) cells and LGN (postsynaptic) cells, less synaptic learning occurs when V1 cell activity is low. Hence, the adaptive synapses weaken less in the feedback pathway from the binocular cell to the right LGN cell (shown as larger synaptic weight in Fig. 7) than in the feedback pathway from the right monocular cell to the right LGN (shown as smaller synaptic weight in Fig. 7). Since a binocular test grating strongly stimulates binocular cells and

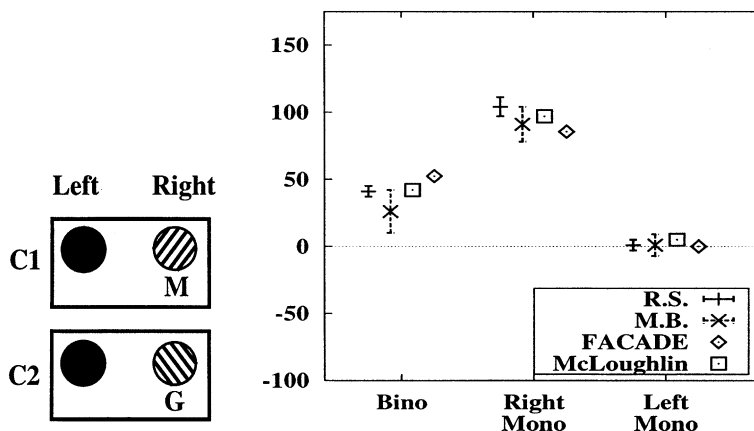


Fig. 6. Standard Monocular Case: (Left) Adapting stimuli used. (Right) Experimental data and simulation results for the McLoughlin and FACADE models.

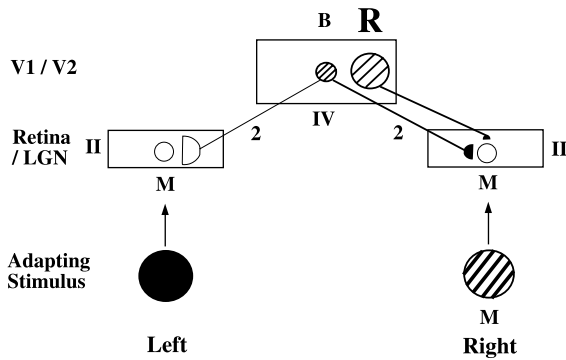


Fig. 7. Schematic diagram of corticogeniculate learning in the model in response to right monocular adaptations with a 45° grating of magenta and black stripes. Illustration follows the conventions used in Fig. 3. The right monocular adapting grating elicits: (1) transmitter habituation in the right LGN; and (2) a strong activation of the right monocular cell (denoted by large R), a weak activation of the binocular cell (denoted by small B), and no activation of the left monocular cell (denoted by an absence of L). Therefore, the pathway from the right monocular cell to the right LGN shows a larger amount of learning (expressed as a larger weakening in synaptic strength), the pathway from the binocular cell to the right LGN shows a smaller amount of learning (expressed as a smaller weakening in synaptic strength), and the pathway to the left LGN shows no learning (expressed as no change in synaptic strength). See text for details.

weakly stimulates monocular cells, the binocular test strongly recruits the smaller magnitude of synaptic learning in the binocular feedback pathway and weakly recruits the larger magnitude of synaptic learning in the right monocular feedback pathway. The right monocular test, on the other hand, strongly recruits the larger magnitude of synaptic learning in the right monocular feedback pathway and weakly recruits the smaller magnitude of synaptic learning in the binocular feedback pathway. Therefore, the binocular test yields a weaker

aftereffect than the right monocular test does, after right monocular adaptation.

3.3. Monocular same case

In the Monocular Same Case, the two eyes are adapted to the same monocular adapting gratings. A pair of such gratings of opposite color and orientation is sequentially alternated. Fig. 8 summarizes the stimuli and results. Comparing the results from the Monocular Same Case with the Standard Monocular Case, it can be seen that the monocular test scores are about the same in both cases, but the binocular test score is greater in the monocular same case than in the standard monocular case. This difference arises in the model because, the feedback pathways projecting to both the left and the right LGN are learned in the Monocular Same Case, whereas only the feedback pathways projecting to the right LGN are learned in the Standard Monocular Case. Therefore, after opponent processing, a binocular test in the Monocular Same Case elicits monocular color signals from both eyes, whereas a binocular test in the Standard Monocular Case elicits monocular color signals from the right eye only. After binocular summation, binocular color signals become greater in the Monocular Same Case than in the Standard Monocular Case. Accordingly, the binocular test score becomes greater in the Monocular Same Case than in the Standard Monocular Case.

3.4. Monocular opposite case

In the Monocular Opposite Case, the two eyes are adapted to opposite monocular adapting gratings. A pair of such gratings of opposite color and orientation is

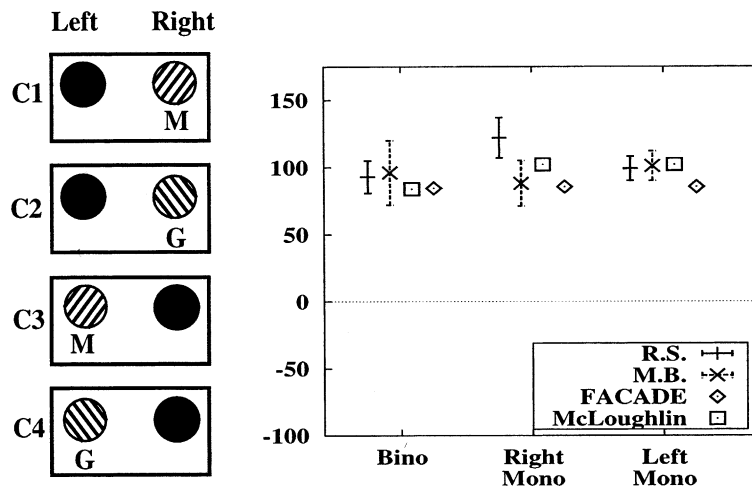


Fig. 8. Monocular Same Case: (Left) Adapting stimuli used. (Right) Experimental data and simulation results for the McLoughlin and FACADE models.

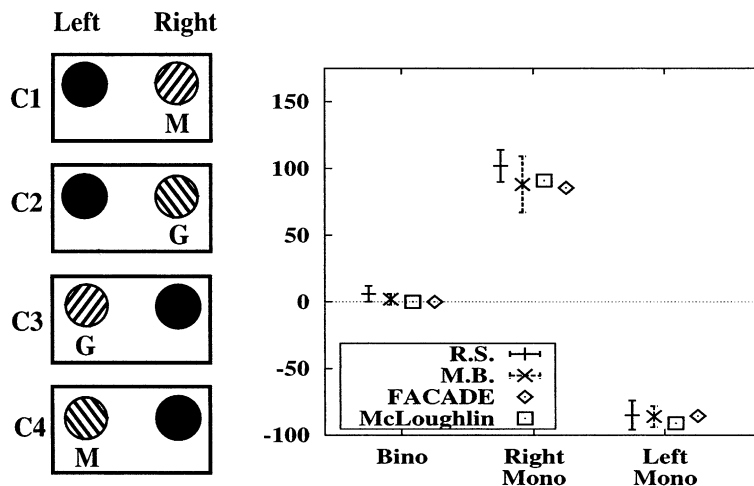


Fig. 9. Monocular Opposite Case: (Left) Adapting stimuli used. (Right) Experimental data and simulation results for the McLoughlin and FACADE models.

sequentially alternated. Fig. 9 summarizes the stimuli and results. As shown in Fig. 9, the binocular test score is around zero and the two monocular tests yield opposite effects. The left monocular test score is plotted on the negative axis to emphasize that the aftereffect color in the left test is opposite to the color in the right test. The present theory explains the opposite monocular test results just as in the Monocular Same Case; namely, using the learning mechanism in the feedback pathways. The monocular aftereffects in the Monocular Opposite Case exhibit opposite colors because the feedback pathways projecting to the two eyes learn from the transmitter habituation of opposite colors. For example, for the C1 stimulus in Fig. 9, the 45° -tuned feedback pathways to the right LGN learn from habituated magenta activities, whereas for the C3 stimulus in Fig. 9, the 45° -tuned feedback pathways to the left LGN learn from habituated green activities. Therefore, testing the right eye with a 45° achromatic grating elicits a green aftereffect, whereas the left monocular test elicits a magenta aftereffect. The same explanation holds for the zero binocular test score. Upon a binocular test with a 45° achromatic grating, green and magenta monocular signals are generated from the right and left eye, respectively. These oppositely colored monocular signals cancel out when they are binocularly summed and opponently processed (Fig. 2, Pathway 6).

3.5. Binocular and monocular opposite case

This case replicates an experiment of Vidyasagar (1976), who was the first to demonstrate that a binocular locus is involved in the ME by showing that the binocular aftereffect can be made opposite to the monocular aftereffect. In this experiment, the two eyes are adapted not only to monocular adapting gratings, but also to

binocular adapting gratings whose colors are opposite to that of the monocular adapting gratings. A pair of these gratings of opposite color and orientation is presented. Fig. 10 summarizes the stimuli and results.

As shown in Fig. 10, the binocular test and the two monocular tests yield small aftereffects even though the adaptation period is made much longer, employing six adapting stimuli. The effects are small in the model because, for each orientation, BCS cells learn the transmitter habituation of both colors whose learned effects subsequently compete with each other via opponent processing, leading to smaller net aftereffects. For example, for stimuli C1 and C4 in Fig. 10, BCS cells tuned to 45° learn from habituated magenta activities, whereas for the C3 stimulus, the same BCS cells learn from habituated green activities. Opponent processing of the two opposite learned effects results in smaller net aftereffects.

The binocular and monocular effects also tend to be opposite because the binocular cells learn more strongly from the color of the binocular adapting gratings, and the monocular cells learn more strongly from the color of the monocular adapting gratings. For example, 45° -tuned binocular cells learn strongly from habituated green activities (the binocular C3 stimulus) and weakly from habituated magenta activities (the monocular C1 and C4 stimuli). Therefore, a binocular test with 45° test grating tends to yield a small magenta aftereffect because binocular test strongly recruits binocular cells. Likewise, a monocular test with 45° test grating tends to yield a small green aftereffect.

It should be noted, however, that the tendency for binocular and monocular tests to yield opposite aftereffects depends on the parametric values of binocular and monocular BCS cells. It is true that, regardless of parametric values, binocular cells learn more strongly

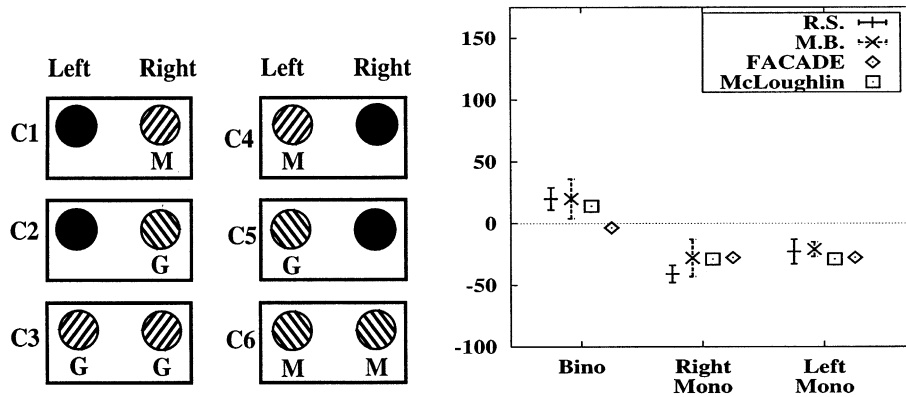


Fig. 10. Binocular and Monocular Opposite Case: (Left) Adapting stimuli used. (Right) Experimental data and simulation results for the McLoughlin and FACADE models.

from the binocular adaptation color than from the monocular adaptation color, and monocular cells learn more strongly from the monocular adaptation color than from the binocular adaptation color. In other words, as far as adaptation and learning are concerned, binocular and monocular cells themselves learn more preferentially from the two opposite colors, regardless of their parametric values. This is because of the constraints that $B_B > B_M$ (binocular cells are more active under binocular stimulations than monocular stimulations), $M_M > M_B$ (monocular cells are more active under monocular stimulations than binocular stimulations).

Aftereffects elicited by binocular and monocular tests, however, do depend on the parametric values of binocular and monocular BCS cells under binocular and monocular stimulation conditions. If BCS cells were exclusive (e.g., binocular stimulations activate binocular cells, but not monocular cells, and vice versa), binocular test would yield an aftereffect complementary to binocular adapting color and monocular test would yield an aftereffect complementary to monocular adapting color, regardless of parametric values. Since BCS cells are not exclusive, however, it is necessary to take into account the activities of the two types of BCS cells under the two types of stimulation conditions. Therefore, aftereffects are parameter-dependent. For example, strong M_M (monocular cell activity under monocular stimulations) and B_M (binocular cell activity under monocular stimulations) causes strong learning during monocular adaptation and strong recruitment of BCS cells during monocular test. In such case, monocular adaptational effects outweigh binocular adaptational effects, leading to a very small binocular test score which may not be opposite to monocular test scores, as shown in Fig. 10. This small deviation of simulations from experimental data is a parametric problem which occurs when fitting data from multiple cases with one set of parameters. It just indicates that, under the current set of parameters,

monocular adaptational effects outweigh binocular adaptational effects for this particular case. Evidence for the hypothesized role of binocular adaptation can be easily observed in the next case.

In this case, investigations are done on how the strengths of the binocular and monocular aftereffects are influenced by longer binocular adaptations while leaving the monocular adaptations the same, by presenting the same binocular adapting gratings twice as long. Fig. 11 summarizes the stimuli and results. By comparing Fig. 11 to 10, it can be seen that longer binocular adaptations result in changes in both binocular and monocular tests. In both tests, changes are observed in an upward direction, which means that binocular adaptational effects begin to outweigh monocular adaptational effects. The observation that the binocular aftereffect becomes stronger under longer binocular adaptations is consistent with our explanation of the Standard Binocular Case, where longer adaptations cause longer activation and learning of BCS cells. The observation that the monocular aftereffect reverses its sign from Fig. 10 to 11 indicates that the effects of longer binocular adaptations eventually predominate over the effects of relatively shorter monocular adaptations. This observation that monocular aftereffects are influenced by longer binocular adaptations to the opposite color provides strong evidence for opponent color processing, and for the activation of binocular cells by monocular inputs. In other words, the binocular cells should act like “OR” gates. This case also provides evidence that the small deviation of simulations from experimental data observed in the previous case is purely a parametric problem. In the previous case (Fig. 10), the deviation indicates that, under the current set of parameters, monocular adaptational effects outweigh binocular adaptational effects. With longer binocular adaptations in the present case (Fig. 11), binocular adaptational effects now outweigh monocular adaptational effects, fitting the experimental data well.

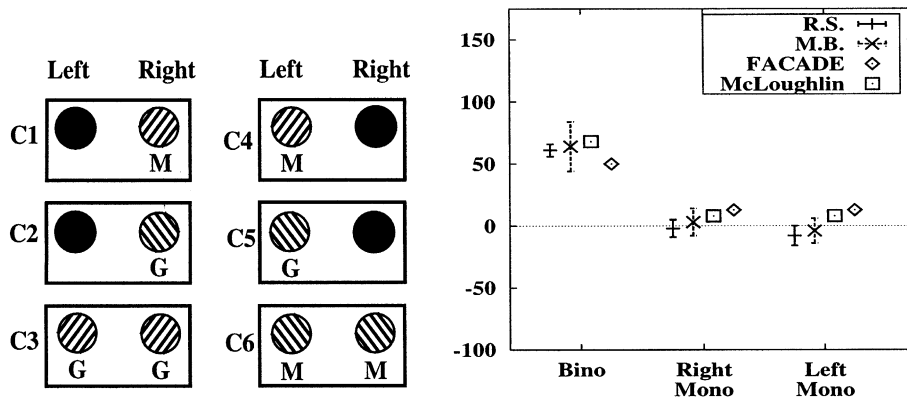


Fig. 11. Binocular and Monocular Opposite Case with Longer Adaptation: (Left) Adapting stimuli used. The same adapting stimuli as in the Binocular and monocular opposite case are used whereas the binocular adaptation period is made twice as long. (Right) Experimental data and simulation results for the McLoughlin and FACADE models.

3.6. Anomalous ME case

The Anomalous ME Case replicates an experiment of MacKay and MacKay (1973), who showed that the ME can be generated by presenting color and orientational information separately to the two eyes. The left eye is adapted to a sequentially alternating pair of homogeneous colored fields. The right eye is adapted to a sequentially alternating pair of achromatic gratings. Fig. 12 summarizes the stimuli and results. The absence of a McLoughlin simulation in Fig. 12 indicates that the McLoughlin model cannot explain the anomalous ME because the color system in the McLoughlin model is strictly monocular; hence, interocular transfer of color information cannot occur. The extra degrees of freedom that are needed to binocularly align and fuse monocular color signals to form a final binocular percept in the FACADE model make it harder to simulate all the cases with a single set of parameters.

As shown in Fig. 12, chromatic aftereffects are induced even though neither of the two eyes was given an

adapting stimulus containing both orientation and color information. Therefore, in this experiment: (1) orientation information transferred from the right eye to the left eye; and (2) color information transferred from the left eye to the right eye. Moreover, the right monocular test yields an anomalous aftereffect (plotted on the negative axis)—that is, its aftereffect was the same hue as the adapting colored field—whereas the left monocular test yields a standard ME. The model explanation of these effects illustrated in Fig. 13.

How does the orientation transfer from the right eye to the left eye, eliciting the standard effect from the color-adapted left eye? This arises in the model because the BCS stage is binocular (i.e., binocular BCS cells act as “OR” gates). The achromatic grating presented to the right eye activates not only the right monocular BCS cell (labeled as “R” in Fig. 13), but also the binocular BCS cell (labeled as “B” in Fig. 13). The feedback pathways projecting from the activated binocular BCS cell to the left magenta LGN then learn from the transmitter habituation in the left eye (shown as a weakened synaptic

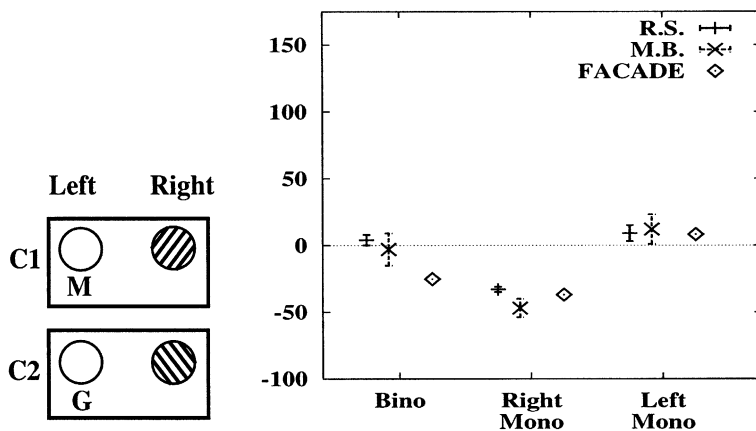


Fig. 12. Anomalous ME Case: (Left) Adapting stimuli used. (Right) Experimental data and simulation results for the FACADE model. The right test yields an anomalous effect, and the left test yields a standard effect.

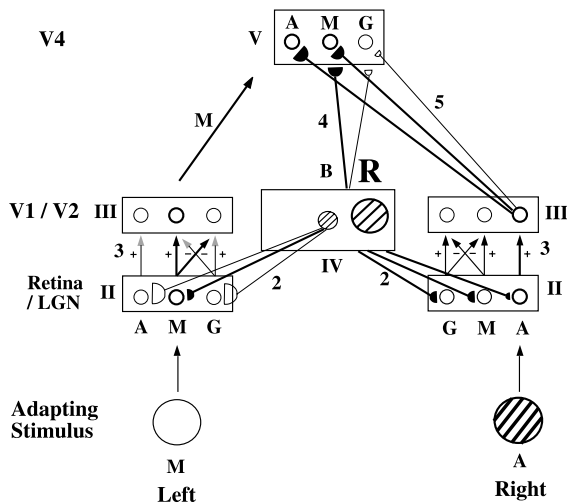


Fig. 13. Schematic diagram of corticogeniculate, cortical bottom-up FCS, and binocular boundary learning in the model in response to C1 adapting stimulus of the Anomalous ME Case. Illustration follows the conventions used in Figs. 3 and 7. In response to the achromatic grating to the right, the binocular cell is activated weakly and the right monocular cell is activated strongly. The corticogeniculate feedback pathway from the binocular cell to the left magenta LGN learns from magenta habituation. The homogeneous magenta stimulus to the left also provides magenta signals to the binocular FIDO (illustrated as an “M” arrow from Stage III in the left to Stage V). The achromatic grating to the right activates the right achromatic cell in Stage III. The cortical bottom-up FCS pathway from the activated right achromatic cell to the binocular magenta cell is learned (illustrated as a strengthening of synaptic strength). The binocular boundary pathway from the activated BCS cells to the binocular magenta cells is also learned (illustrated as a strengthening of synaptic strength). Both the learning in the cortical bottom-up FCS pathway and the binocular boundary pathway are involved in the anomalous ME.

weight in that pathway in Fig. 13). Therefore, orientation information can transfer interocularly, and this case provides additional evidence that the binocular cells act as “OR” gates. The left test score is nevertheless weak in the model because of two reasons. First is the “dilution” of the aftereffect by recruiting the left monocular BCS cell during test, whose feedback pathway did not learn during adaptation. The second reason comes from the proposal that binocular cells are less active during monocular stimulations than during binocular stimulations (shown as smaller “B” compared to larger “R”). Therefore, the magnitude of learning in the feedback pathway from the binocular BCS cell to the left LGN is small, which then leads to the smaller aftereffect in the left monocular test.

How does the color transfer from the left eye to the right eye, eliciting the anomalous effect from the orientation-adapted right eye? This arises in the model by: (1) the binocular FCS stage (Fig. 13, Stage V) where monocular color signals from the two eyes are combined; and (2) the learning in the two adaptive pathways to the binocular FCS—the cortical bottom-up FCS pathway

(Fig. 13, Pathway 5) and the binocular boundary pathway (Fig. 13, Pathway 4).

Both pathways learn with the same mechanisms that are used for the corticogeniculate feedback pathway; namely, synaptic learning takes place only when both presynaptic and postsynaptic cells are concurrently active, and synaptic strength tracks postsynaptic activity. In the case of the cortical bottom-up FCS pathways, the presynaptic cells are monocular FCS cells and the postsynaptic cells are binocular FCS cells. In the case of the binocular boundary pathways, the presynaptic cells are BCS cells and the postsynaptic cells are binocular FCS cells.

In response to the C1 adapting stimulus, achromatic cells in the right monocular FCS (shown as cell “A” of Stage III in Fig. 13), which are normally connected to achromatic cells in the binocular FCS, become associated also with magenta cells in the binocular FCS (shown as a learned synapse in the pathway from cell “A” of Stage III to cell “M” of Stage V in Fig. 13) which are activated by magenta stimulations in the left eye. As this association between monocular and binocular color signals grows, 45°-tuned binocular boundary pathways to the magenta cells in the binocular FCS also grow (shown as a learned synapse in the binocular boundary pathways to cell “M” of Stage V in Fig. 13), due to correlation between orientation and binocular color. Likewise, in response to the C2 adapting stimulus, the right monocular achromatic cells become associated also with binocular green cells, and 135°-tuned binocular boundary pathways to green cells in the binocular FCS become stronger. This correlated binocular boundary learning leads to preferential gating of a color signal which has been correlated with a given orientation, over the other color signal which has not been correlated.

For example, magenta and green FCS signals of equal strength are elicited in the binocular FCS upon a right test, due to prior learning within the cortical bottom-up FCS pathway during C1 and C2. Due to orientation-selective boundary gating, when a 45° test grating is used, magenta FCS signals are more strongly gated than green FCS signals, leading to stronger magenta filled-in activities than green filled-in activities. Net magenta activities are obtained upon binocular opponent processing, which correspond to the anomalous ME. The opposite is true for a right test with a 135° test grating. In short, the cortical bottom-up pathway learns the correlation of a right achromatic FCS signal and binocular FCS chromatic signals, and the binocular boundary pathway learns the correlation of an orientation and a binocular FCS chromatic signal.

Even though the same learning law is used in both the corticogeniculate feedback pathway and the binocular boundary pathway, the former become weakened whereas the latter become strengthened during

adaptation. How do these opposite learning effects happen? The model proposes that this is due to the nature of the ongoing learning and decay which adaptive pathways in the model are conceptualized to undergo. In the simulations, synaptic weights of these pathways are set up during the weight-initialization phase, as described earlier. Under normal viewing conditions, correlations between monocular *achromatic* FCS signals in one eye and monocular *chromatic* FCS signals in the other eye are very small at the binocular FCS. The anomalous ME stimuli force these correlations to grow, and the correlations from boundary cells to the binocular FCS grow correspondingly. In contrast, the corticogeniculate boundary-to-(monocular FCS) signals start out large, and weaken due to prolonged stimulus inspection. In order to implement these differential correlations in a simple way, training stimuli were presented continuously to the network during the weight-initialization phase, and the corticogeniculate feedback pathway was learned until equilibrium was reached. In contrast, learning in the binocular boundary pathway to the FCS was stopped in the middle of learning (at the 50th iteration of numerical integration).

In summary, aftereffects can be elicited even when color and orientation information are presented separately to each eye. The color-adapted eye shows a normal aftereffect in the model because the color of one eye can be correlated with the orientation transferred from the other eye, and this interocular transfer of orientation arises at the binocular BCS. The orientation-adapted eye shows an anomalous aftereffect in the model because the orientation of one eye can be correlated with the color transferred from the other eye, and this interocular transfer of color arises at the binocular FCS. On the other hand, the ME does not transfer interocularly under monocular adaptation (see Fig. 6) because the unadapted eye is presented with neither color nor

orientation, hence the adaptive pathways in the unadapted eye are not learned.

3.7. Monocular adaptation with white field occlusion

The Standard Monocular Case showed that aftereffects do not transfer interocularly when the unadapted eye is occluded with a black field. Lehmkuhle and Fox (1976) reported that the magnitude of interocular transfer of a motion aftereffect was influenced by the method that was used to block stimulation of unadapted eye. In particular, less interocular transfer was produced by occluding the unadapted eye with a dark field than with a homogeneous luminous field. For this reason, they speculated that occluding the unadapted eye with an achromatic luminous field might reveal interocular transfer in those kinds of aftereffects where transfer had not been previously reported. This possibility was investigated by McLoughlin (1995), who used an achromatic luminous field, rather than a black field, to occlude the unadapted eye. The left eye was adapted to a white luminous field and the right eye to a pair of sequentially alternating monocular gratings of opposite color and orientation. Fig. 14 summarizes the stimuli and results.

As shown in Fig. 14, testing the unadapted left eye yielded a nearly zero aftereffect, just as in the standard monocular case. The absence of interocular transfer arises in the model because the white field results in equal habituation within the magenta and green LGN cells. Therefore, the corticogeniculate feedback pathway learning of these equal but opposite habituations is also equal in magnitude. After opponent processing, these equal and opposite effects cancel out. Since interocular transfer is not observed both from the Standard Monocular Case and the present case, it can be said that the interocular transfer of the ME is not influenced by the

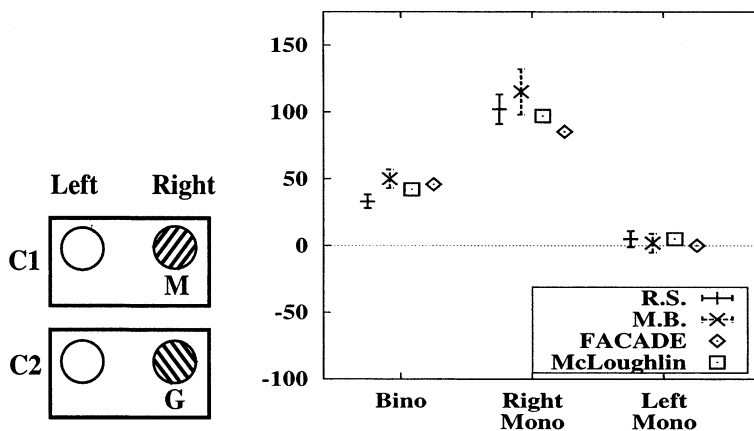


Fig. 14. Monocular Adaptation with White Field Occlusion case: (Left) Adapting stimuli used. (Right) Experimental data and simulation results for the McLoughlin and FACADE models.

occlusion method, contrary to the Lehmkuhle and Fox (1976) speculations.

Quantitative analyses showed that, unless further assumptions were made, learning tended to yield a small anomalous effect, rather than a zero aftereffect, when the left eye was tested. This tendency occurred in the present case because one eye is presented with achromatic color and the other eye with chromatic color. As in the anomalous ME case, this type of stimulus presentation would associate monocular achromatic cells with binocular chromatic cells. As this association grows, boundary learning would correlate an orientation and a binocular color. Subsequent test with an achromatic grating would cause preferential gating of a color signal that has been correlated with a given orientation, over the color signal which has not been correlated, eliciting an anomalous effect when the achromatically adapted eye is tested. The effect would be small in the present case because the achromatically adapted left eye did not receive an orientation signal, hence its boundary pathway did not learn; only the learned boundary from the weakly activated binocular BCS cell is recruited.

We speculate that this tendency may be an artifact. Two assumptions that incorporate properties of the connections which may be expected to develop due to real-world properties of images enable the model to successfully explain the present case while preserving the fit for all other cases. In brief, the two assumptions help to cause little association between monocular achromatic cells and binocular chromatic cells in the present case, but significant association between monocular achromatic cells and binocular chromatic cells in the Anomalous ME Case, as desired.

The first assumption is that association between monocular and binocular FCS cells occurs weakly when they code different color. For example, learning from monocular achromatic to binocular chromatic cells is weaker than from monocular achromatic to binocular achromatic cells. This assumption is intuitive because a key function of the adaptive mechanisms in the cortical bottom-up FCS pathway is to establish and to maintain selective contacts between monocular FCS cells and binocular FCS cells that code the same spatial positions and color. Since the two eyes are presented with the same color during normal viewing conditions, anatomical connections between cells that code different color should be weak and sparse. Therefore, when the two eyes are presented with different colors as in the present case (white to the left eye, color to the right eye), the cortical bottom-up FCS pathway learns weakly, and a spurious anomalous aftereffect will not be elicited in the left test in the present case.

Given these weaker anatomical cross-connections, how is an anomalous aftereffect elicited in the Anomalous ME Case? One additional assumption helps to explain all the data. It constitutes a prediction for which

some compatible data are known, but does not seem to have been directly tested. This assumption is that achromatic channels adapt less than chromatic channels. Thus, in response to anomalous ME stimuli, the achromatic channel adapts weakly, because there is less habituation in its transmitters. As a result, learned corticogeniculate feedback to the right achromatic FCS cell weakens less (Fig. 13, Pathway 2), so that the right achromatic signals yield larger outputs (Fig. 13, Cell A of Stage III). The stronger monocular FCS cell activity causes faster learning in the cortical bottom-up FCS pathway. Thus, the cortical bottom-up FCS pathway from right achromatic cells to binocular chromatic cells (Fig. 13, Pathway 5) shows considerable learning despite its weaker anatomical connections, thus eliciting an anomalous aftereffect.

There are many possible ways in which achromatic and chromatic channels can differ, including the input ranges that they encode and their temporal dynamics. For simplicity, in the simulations, achromatic and chromatic LGN cells were given the same rate parameters, and the differential adaptational property was implemented by a smaller transmitter inactivation rate (μ_1 of Eq. (13) in Appendix A) in the achromatic LGN cells than in the chromatic LGN cells. There is evidence that rods show less change than cones during adaptation by steady light (Cohn & Lasley, 1986), but little data about whether more central mechanisms also show this predicted difference.

3.8. Like color case

This case replicates the “like color” experiment of White et al. (1978). The left eye is adapted to a sequentially alternating pair of homogeneous colored fields. The right eye is adapted to a sequentially alternating pair of colored gratings of like colors. Fig. 15 summarizes the stimuli and results. A main finding of this case is that, even though the left adapting stimuli are devoid of orientational information, the aftereffect is nevertheless observed in the left eye, although the strength of the aftereffect is small. It indicates that orientational information can transfer interocularly. This arises in the model because the BCS stage is binocular, as described earlier for the model explanation of how the color-adapted eye can show a standard aftereffect in the Anomalous ME Case.

3.9. Different color case

This case replicates the “different color” experiment of White et al. (1978) and is identical to the Like Color Case except that the two eyes see different colors in this case. Fig. 16 summarizes the stimuli and results. As shown in Fig. 16, a main finding of this case is that the left monocular test yields a zero aftereffect. This effect is

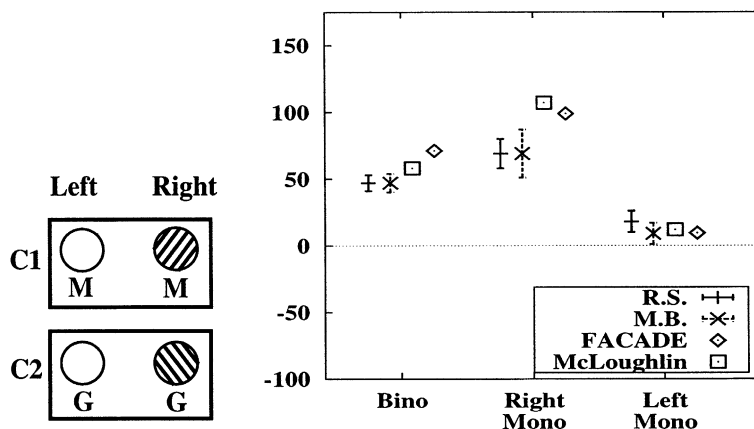


Fig. 15. Like Color Case: (Left) Adapting stimuli used. (Right) Experimental data and simulation results for the McLoughlin and FACADE models.

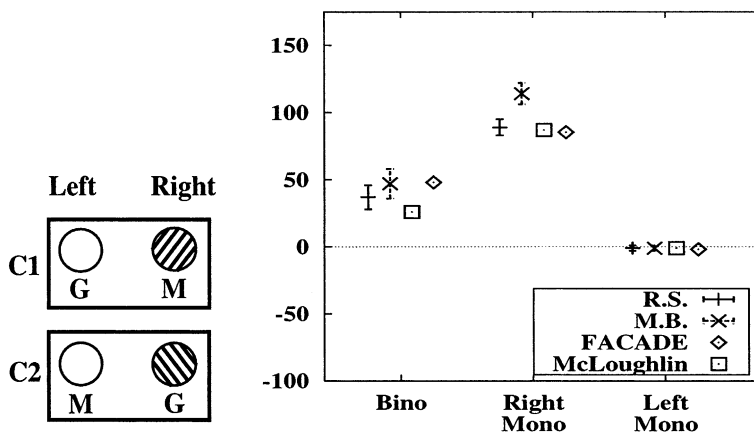


Fig. 16. Different Color Case: (Left) Adapting stimuli used. (Right) Experimental data and simulation results for the McLoughlin and FACADE models.

explained in the model by combining the adaptive mechanisms of the corticogeniculate feedback pathway and of the cortical bottom-up FCS pathway. As has been explained previously in the Anomalous ME Case and the Like Color Case, the orientational information of adapting stimuli transfers interocularly by virtue of binocular boundary cells which can trigger corticogeniculate feedback learning. For example, in response to the C1 stimulus in Fig. 16, learning in the feedback pathway from binocular boundary cells to left green LGN cells would lead to a small magenta aftereffect in the left eye. However, such an effect is not observed in the present case because the learning in the cortical bottom-up FCS pathway cancels it out.

This cancellation happens in the FACADE model as follows. As has been explained in the Anomalous ME Case, magenta and green cells in the monocular FCS are normally connected to magenta or green cells, respectively, in the binocular FCS. The dichoptic adaptation to two different colors in the present case, however, retunes these connections such that magenta and green

cells in the monocular FCS become, to a certain degree, cross-associated to green and magenta cells in the binocular FCS, respectively. This cancels out the small magenta effect produced by the feedback learning in response to the C1 stimulus at the left LGN, resulting in a nearly zero aftereffect in the left monocular test, as shown in Fig. 16. To summarize, the learning in the corticogeniculate feedback learning and in the cortical bottom-up FCS pathway compete with each other in the present case.

3.10. Isoluminant adaptation case

This case replicates an experiment of Stromeyer and Dawson (1978) and is identical to the standard binocular case except that the gratings are made of isoluminant colored and gray stripes. Fig. 17 summarizes the stimuli and results. As Stromeyer and Dawson (1978) have shown, the use of isoluminant adapting gratings fails to induce the ME. This arises in the model because BCS cells are assumed to be inactive in response to

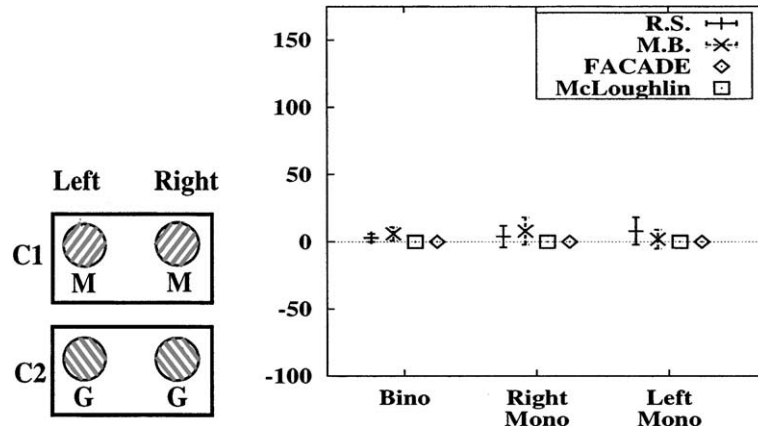


Fig. 17. Isoluminant Adaptation Case: (Left) Adapting stimuli used. (Right) Experimental data and simulation results for the McLoughlin and FACADE models.

isoluminant stimuli, which is consistent with the Savoy (1987) discussion suggesting that only the luminance contrast information is used in the processing of orientation and edges during the ME. Since BCS cells are not active, learning does not occur in the corticogeniculate feedback pathway; hence, aftereffects are not induced.

3.11. Binocular rivalry case

This case replicates the “different color/different orientation” experiment of White et al. (1978). In this case, the two eyes are adapted to opposite binocular adapting gratings. A pair of such gratings of opposite color and orientation is sequentially alternated. Fig. 18 summarizes the stimuli and results. As shown in Fig. 18, standard aftereffects are observed in both the binocular and the monocular tests although the two eyes see different orientation/color combinations during adaptation. This is explained in the model using the learning mechanisms in the corticogeniculate feedback pathway; namely, the corticogeniculate feedback pathway learns the correla-

tion of an orientation and a habituated monocular color signal, which are used in explaining all other cases throughout this article.

As shown in Fig. 18, the two eyes are presented with opposite orientation/color combinations at any given time. During adaptation with C1 stimulus, for example, the left eye is presented with a 135° green grating and the right eye is presented with a 45° magenta grating. The opposite is true for adaptation with a C2 stimulus. When both C1 and C2 adapting stimuli are taken into account together, however, it can be seen that both the left and the right eye are adapted to the same color at any given orientation. For example, the magenta grating is 45° in orientation, whereas the green grating is 135° in orientation. Therefore, 45°-tuned feedback pathways to the left and the right LGN learn from habituated magenta activities, and 135°-tuned feedback pathways to the left and the right LGN learn from habituated green activities. Thus, tests yield standard aftereffects: tests with a 45° test grating elicit a green aftereffect and tests with a 135° test grating elicit a red aftereffect, even

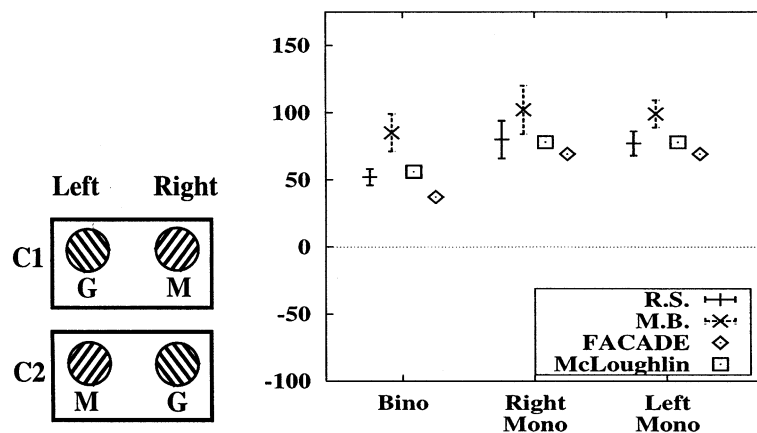


Fig. 18. Binocular Rivalry Case: (Left) Adapting stimuli used. (Right) Experimental data and simulation results for the McLoughlin and FACADE models.

though the two eyes see different orientation/color combinations during adaptation.

Previous work on FACADE theory (Grossberg, 1987) has noted how dichoptically presented stimuli whose orientations are perpendicular to each other can give rise to a rivalrous competition between two subpopulations of binocular BCS cells that are tuned to perpendicular orientations. For simplicity, the habituating mechanisms that drive boundary rivalry are not implemented here. In the simulations, this property is implemented by reducing the activities of binocular BCS cells to 75% of normal activity, but leaving the activities of monocular BCS cells unaffected. This is consistent with the study of Sengpiel, Blakemore, and Harrad (1995) who investigated the responses of cat area 17 neurons to study the neural mechanisms responsible for binocular rivalry. By stimulating the two eyes with two gratings oriented perpendicular to each other, they showed that only the binocular neurons were suppressed by the rivalrous stimuli and proposed that the suppressed behavior of the binocular neurons plays a role in binocular rivalry.

4. Discussion

The present article models how the ME, which is a long-lasting, orientation-contingent complementary color aftereffect, arises. We predict that it occurs as an emergent property when visual learning mechanisms, whose primary role is to adaptively align boundary and surface representations, interact with habituating transmitter gates in chromatic opponent-processing circuits. Our analysis clarifies why interocular transfer of the ME does not occur under monocular adaptation even though various interocular properties of the ME are known to exist (Vidyasagar, 1976; White et al., 1978), and notably how the anomalous ME occurs (MacKay & MacKay, 1973). We explained these seemingly conflicting observations by positing multiple learning sites: (1) the pathway connecting the binocular BCS to the monocular FCS; (2) the pathway connecting the monocular FCS to the binocular FCS; and (3) the pathway connecting the binocular BCS to the binocular FCS. In the architecture of the present model, the corticogeniculate feedback pathway was suggested as a possible site to implement the model pathway from the binocular BCS to the monocular FCS. The model, however, could also be interpreted to explain ME data using the pathway from the binocular BCS to the monocular FIDO. The monocular FIDO is a filling-in stage where featural signals from a single eye are captured in depthful representations by binocular BCS signals. This process has been used to explain data about figure-ground perception and stereopsis (Grossberg, 1994, 1997; Grossberg & McLoughlin, 1997). It was simplified in the present

model to become Stage III in Fig. 2. A possible site for the monocular FIDO in vivo is the thin stripes of cortical area V2 (Grossberg, 1997). The model is able to simulate the present data using such an alternative interpretation because the (binocular BCS)-to-(monocular FIDO) pathway connects the binocular BCS to the monocular FCS, just as the corticogeniculate feedback pathway does.

As described earlier in this article, interocular properties of the ME have not received much theoretical attention. Although there have been two models that describe those properties of the ME (McLoughlin, 1995; Savoy, 1984), they did not offer even a descriptive explanation of the anomalous ME data of MacKay and MacKay (1973), since the color systems in their models were exclusively monocular.

Interocular transfer of the ME does not occur under monocular adaptation in the present model because LGN cells in the unadapted eye are not activated; hence, learning does not occur in the corticogeniculate feedback pathways projecting to the unadapted eye. On the other hand, interocular effects of both orientation and color are observed, providing that partial information about color or orientation is given, as in the Anomalous ME Case (a color to one eye, an orientation to the other eye), in the Like Color Case (a color to one eye, an orientation and the same color to the other eye), and in the Different Color Case (a color to one eye, an orientation and the opposite color to the other eye).

Orientation information transfers interocularly in the model by the binocular BCS. Thus a normal aftereffect can be elicited from the color-adapted eye, and it was demonstrated in the Anomalous ME Case (the left test) and the Like Color Case (the left test). Color information transfers interocularly in the model by the binocular FCS. Thus an anomalous effect can be elicited from the orientation-adapted eye, and it was demonstrated in the Anomalous ME Case (the right test). Interocular effects of color were also simulated such that the eye adapted with a homogeneously colored field fails to exhibit the effect in the Different Color Case. The model explains this in terms of the learning in the cortical bottom-up FCS pathway that competes with the effect of the learning in the corticogeniculate top-down pathway, which would otherwise exhibit a standard ME.

In the present article, we have focused on how adaptive mechanisms in the nervous system generate changes in neural loci that subserve the ME as their perceptual outcome. There have been several other theoretical attempts to do this. Some of them suggested that the ME arises from the fatigue of neurons that are tuned to both orientation and color (McCullough, 1965; Michael, 1978). Some “double-duty” neurons that are tuned to both orientation and color are, indeed, found in monkey visual cortex (Michael, 1978). However, there have been numerous discussions that models based on

simple fatigue alone cannot provide an explanation for the ME (e.g., see Jones & Holding (1975), MacKay & MacKay (1975)).

Others have suggested that the persistence of the ME arises from synaptic changes in the connection between neurons for orientation and neurons for color (McLoughlin, 1995; Murch & Hirsch, 1972; Savoy, 1984). These models were also incomplete, however, because they were not able to explain the anomalous ME data of MacKay and MacKay (1973), where there was interocular effects of color information. Also these models did not give a functional rationale for why such adaptive pathways are needed during normal vision.

The model of McLoughlin (1995) incorporated a number of FACADE mechanisms, such as learning of transmitter-habituated signals and opponent processing. As noted in Section 1, the McLoughlin model also differs from the present model in several ways: (1) the model is not spatially distributed; (2) there is no mechanism, such as filling-in, for generating a visible surface percept. Rather, the network output is derived simply by averaging monocular color signals, which are additively influenced by learned weights; (3) its orientation system additively influences chromatic system activity, rather than multiplicatively, as in the present model. Thus, an oriented input to one eye alone can activate monocular chromatic cells in the other eye, even in the absence of retinal input to the latter eye; and, (4) there are no processing stages for binocular color, which prevent it from explaining interocular properties of the ME. Proposals for how to overcome these problems are developed in the present version of the FACADE model.

Another class of theories does focus on the functional importance of the ME. In some of these theories, the ME is proposed to arise from a process of correcting errors and biases that are imposed during adaptations in ME experiments. For example, Shute (1979) suggested that the abnormal correlations between pattern and color induced by adapting gratings are recorded in the hippocampus. When the pattern is subsequently presented alone during test trials, an inhibitory mechanism in the hippocampus was proposed to inhibit neurons for the adapting color and to disinhibit neurons for the opponent color, resulting in the perception of a complementary color. Evidence for such a hippocampal process seems to be lacking, including evidence for cells with these featural properties.

Dodwell and Humphrey (1990) proposed that the presentation of, for example, a red vertical adapting grating will shift the “neutral point” for red-vertical correlations towards the red side of the color space. The shift occurs because a hypothesized mechanism, called an “error correcting device”, is at work in order to maintain a color-pattern neutrality. After the shift, an achromatic vertical test grating would appear greenish because an achromatic light, which was a neutral point

prior to adaptation, now belongs to the green side of the shifted color space. A similar argument is found in the Warren (1985) proposal of a “criterion shift rule”. Bedford (1993, 1995) also suggested that the ME arises in order to correct a perceptual error that arises when there is a violation of a perceptual constraint that an object should not change its color when it is rotated, since the presentation of a pair of adapting gratings of opposite color and orientation can be interpreted as a change in color of a single object that is rotated 90°. The unit of learning in the Bedford model is, therefore, two patterns. As discussed in Allan and Siegel (1997) and Bedford (1995, 1997), it is not yet clear how the Bedford model can be made consistent with aftereffects elicited by a single adaptation pattern (Stromeyer, 1969). Our own explanation of the ME is based on single pattern learning and employs mechanisms that operate at lower cortical levels than those involved in invariant pattern recognition.

In other functional theories (Broerse et al., 1999; Held, 1980; Hohmann & von der Malsburg, 1978), the ME was proposed to arise from neural processes whose normal function is to compensate for chromatic aberration of the eye (Hay, Pick, & Rosser, 1963), which are revealed in experiments where subjects wear prism goggles that differentially bend lights of different wavelengths (Harris, 1980; Kohler, 1962). This type of theory is of particular interest concerning the lack of interocular transfer in the ME because it makes intuitive sense that the compensation processes for chromatic aberrations not be transferred interocularly because the two eyes differ in their aberrations, as Held (1980) noted.

A strong advantage of the present model, apart from the ME data-prediction properties, is that its main concepts and mechanisms were not derived to explain ME data. Rather, they are natural consequences of the FACADE theory prediction that boundaries and surfaces are computed by parallel cortical processing streams, a hypothesis for which there is now a lot of experimental evidence (e.g., Dresch & Grossberg, 1997, 1999; Elder & Zucker, 1998; Lamme, Rodriguez-Rodriguez, & Spekreijse, 1999; Rogers-Ramachandran & Ramachandran, 1998).

Although not simulated here, several other known properties of the ME can also be explained by the present model. It has been shown that the ME can be induced not only by scanning the adapting patterns, but also by fixating them. The induction of the ME during fixation is selective to retinotopy, such that the aftereffect is seen only when the test gratings fall on the same retinal position as the adapting gratings (Stromeyer & Dawson, 1978). The present model can explain the scanning case since adaptive pathways across the visual field adapt equally on the average during scanning. The fixation case can also be explained, since the only pathways that can adapt are those whose retinal

locations of receptive fields lie within the colored stripes of the adapting gratings.

Extinction properties of the ME, which show that the ME decays faster due to viewing of achromatic gratings (Skowbo, Gentry, Timney, & Morant, 1974), can also be explained by the present model. Since achromatic gratings equally activate both the magenta and green LGN cells, any imbalance that was caused by prior color adaptation and learning disappears. The observation that monocular viewing of achromatic gratings does not extinguish a binocularly induced ME of the other eye (Savoy, 1984) is also explained by the model because the achromatic grating seen in the one eye removes the imbalance caused by prior color adaptation only in that eye, but not in the other eye.

The model is also consistent with the data of Skowbo and White (1983), who showed that the acquisition of the ME depends on the duration, not on the number, of induction stimulus presentations. In the present model, the unit of learning is not the number of orientation–color pairings (as proposed by a classical conditioning account), but is the duration of induction stimuli, during which the transmitter habituates and the slowly varying synaptic weight learns. The total amount of habituation covaries with the duration of induction stimuli rather than with the number of stimulus presentations, since the total habituation (i.e., depletion and recovery) is a cumulative process which continues during stimulus presentations. When the alternation rate of induction patterns is increased, for example, not only does more transmitter depletion occur when a pattern turns on, but also more transmitter recovery occurs when the pattern turns off. Therefore, the total transmitter habituation level may remain largely constant when the alternation rate is varied. The slowly varying synaptic change also covaries with the stimulus duration when driven by transmitter habituation. Therefore, the present model can explain why the acquisition of the ME depends on the duration, not on the number, of induction stimulus presentations. Simulations of the habituating process under a number of presentation conditions (not reported here) have confirmed this property of the model.

The time course of the ME establishment can also be qualitatively explained by the present model. Riggs, White, and Eimas (1974) varied the duration of adaptation by roughly equal logarithmic steps ranging from 15 s to 25 min and found that the ME strength showed an approximately linear increase to a logarithmic scale of adaptation period. This is consistent with the slower-than-linear time course of our synaptic learning, where weight changes are initially fast and decelerate as the weight approaches an asymptotic level through time.

In several studies (Jenkins & Ross, 1977; Meyer & Phillips, 1980; Uhlark, Pringle, & Brigell, 1977), test stimuli were perceptually reversible figures composed of horizontal and vertical gratings. After typical induction

procedures with colored vertical and horizontal gratings, the ME was observed only for the organization that segregated vertical and horizontal pattern elements in the test figure. Meyer and Dougherty (1987) asserted that this dependence of the ME on perceptual organization arises from a filling-in process of the type used by the FACADE model. When the vertical and horizontal gratings in the test figure are perceptually segregated, filling-in of the ME hue stops at the subjective contour established by the BCS. The ME cannot be observed on the other organization because the opposite ME hues elicited by vertical and horizontal gratings in the test figure fill-in throughout the perceived region and thus cancel out with each other due to the lack of a subjective contour, as Meyer and Dougherty (1987) noted.

Similarly, Broerse and O'Shea (1995) and Broerse et al. (1999) also conjectured that the ME involves a filling-in process of the type used by the FACADE model, using the two proposed components of the ME: edge colors located at edges of contours, and spread colors that spread away from edge colors in order to fill-in adjacent white stripes of test patterns.

Watanabe (1995) used a test pattern in which white stripes were partially occluded by white surfaces. By means of stereo depth cue, the test pattern was perceived as stripes partially occluded by overlaid surfaces. Even though only part of the stripes were visible, the ME was nevertheless observed. Moreover, the ME was observed only within nonoccluded region of the stripes but not within occluded region. This observation is consistent with the FACADE explanation of Bregman–Kanizsa figure-ground separation and completion (Grossberg, 1994, 1997).

5. Conclusion

In summary, the present article extends the explanatory range of FACADE theory to explain the ME, particularly data concerning how interocular properties of the ME arise. The model explains them as perceptual consequences of visual system mechanisms whose primary role is to establish and maintain a topographic mapping between boundary and surface representations, to compensate for the positional displacement that occurs in the boundary system due to binocular fusion and allelotropia.

Appendix A. Equations and parameters

Simulations are done on a one-dimensional array of 300 units. Unless otherwise stated, differential equations were solved numerically by Euler's method with step size 0.2. Computations were done in the C programming

language with a GNU C compiler on an IBM-compatible PC with a LINUX operating system.

A.1. Retina and LGN cells (Fig. 2, Stage I)

Three types of wavelength-sensitive inputs are modeled at each position i : achromatic (a_i), magenta (m_i), and green (g_i). They are combined as follows to form inputs to the model cells:

$$I_i^a = a_i, \quad (1)$$

$$I_i^m = m_i + \rho a_i, \quad (2)$$

and

$$I_i^g = g_i + \rho a_i, \quad (3)$$

where I_i^a , I_i^m , and I_i^g denote inputs to achromatic, magenta, and green cells, respectively. Eqs. (2) and (3) say that the achromatic input not only activates achromatic cells, but also chromatic cells. This indirect activation of chromatic cells by an achromatic test input is one basis of the ME. Parameter ρ specifies the relative sizes of chromatic and achromatic inputs. For simplicity of notation, Eqs. (2) and (3) can be expressed in a single equation as:

$$I_i^{m|g} = (m_i|g_i) + \rho a_i. \quad (4)$$

This type of notation with the symbol “|” to mean “either or” will be used throughout this paper whenever needed.

Grating inputs are represented as interdigitating one black stripe and two colored stripes of an amplitude of 10.0, presented in a black background. A magenta grating input, for example, is represented as:

$$I_i^m = \begin{cases} 10.0 & \text{if } 75 \leq i < 125 \text{ or } 175 \leq i < 225, \\ 0.0 & \text{otherwise.} \end{cases} \quad (5)$$

Similarly, a homogeneous magenta field is represented as:

$$I_i^m = \begin{cases} 10.0 & \text{if } 75 \leq i < 225, \\ 0.0 & \text{otherwise.} \end{cases} \quad (6)$$

Green and achromatic inputs can be similarly derived from Eqs. (5) and (6).

Since there are two eyes in the system, a general form of input for a given eye and color can be represented as I_i^{ec} , where the superscript ‘e’ (eye) is either ‘l’ (left) or ‘r’ (right), and the superscript ‘c’ (color) is either ‘a’ (achromatic), ‘m’ (magenta), or ‘g’ (green). Hence, chromatic inputs to the left eye, for example, can be expressed as:

$$I_i^{l(m|g)} = (m_i^l|g_i^l) + \rho a_i^l. \quad (7)$$

The activity s_i of the retina/LGN cell at position i obeys a membrane equation:

$$\begin{aligned} \frac{d}{dt} s_i = & -A_1 s_i + (B_1 - s_i) \sum_{k=1}^N I_k C_{1ki} \\ & - (s_i + D_1) \sum_{k=1}^N I_k E_{1ki}, \end{aligned} \quad (8)$$

where N is the number of cells in the system, and the terms $\sum_{k=1}^N I_k C_{1ki}$ and $\sum_{k=1}^N I_k E_{1ki}$ represent on-center and off-surround inputs, respectively. Excitatory (C_{1ki}) and inhibitory (E_{1ki}) on-center and off-surround receptive fields, respectively, are defined by Gaussian kernels:

$$C_{1ki} = C_1 \exp \left[-\frac{1}{\theta_1^2} (k-i)^2 \log 2 \right] \quad (9)$$

and

$$E_{1ki} = E_1 \exp \left[-\frac{1}{\lambda_1^2} (k-i)^2 \log 2 \right]. \quad (10)$$

In the simulations, Eq. (8) is solved at equilibrium so that:

$$s_i = \frac{\sum_{k=1}^N (B_1 C_{1ki} - D_1 E_{1ki}) I_k}{A_1 + \sum_{k=1}^N (C_{1ki} + E_{1ki}) I_k}. \quad (11)$$

The output signal from each cell is half-wave rectified:

$$S_i = [s_i]^+, \quad (12)$$

with $[x]^+ = \max(x, 0)$. As described previously, activities of retina/LGN cells for a given ocularity and color can be obtained by putting appropriate superscripts in Eq. (11).

A.2. Monocular transmitter habituation (Fig. 2, Pathway I)

The transmitter level t_i of the i th retina/LGN cell pathway is described by the following transmitter habituation, or depression equation:

$$\frac{d}{dt} t_i = \eta_1 [L_1 - (1 + \mu_1 S_i) t_i]. \quad (13)$$

where η_1 is a rate constant that governs overall transmitter dynamics (i.e., depletion and recovery), and μ_1 is a rate constant for transmitter depletion. In Eq. (13), transmitter accumulates to target level L_1 at rate η_1 via term $\eta_1 (L_1 - t_i)$, and is inactivated, or released, in an activity-dependent way via term $-\eta_1 \mu_1 S_i t_i$. Transmitter-gated output is proportional to its inactivation rate:

$$T_i = S_i t_i. \quad (14)$$

The same Eqs. (13) and (14) exist for each ocularity and color.

A.3. BCS cells (Fig. 2, Stage IV)

BCS cells are tuned to orientation and ocularity. In the simulations, two orientations (45° and 135°) and three ocularities (left monocular, binocular, and right monocular) are considered. The following four constants describe BCS cell activities: B_B denotes binocular cell activity under binocular stimulation, B_M denotes binocular cell activity under monocular stimulation, M_M denotes monocular cell activity under monocular stimulation, and M_B denotes monocular cell activity under binocular stimulation.

Activities of BCS cells at position j are denoted as A_j . For simplicity, only those BCS cells located at the positions corresponding to edges of input stimuli are activated to one of the four values (B_B, B_M, M_M, M_B). For example, when the network is presented with binocular gratings, activation of binocular BCS cells can be expressed as follows:

$$A_j = \begin{cases} B_B & \text{if } j \in \{75, 125, 175, 225\}, \\ 0.0 & \text{otherwise.} \end{cases} \quad (15)$$

All other cases of activation can be similarly derived from Eq. (15).

Since BCS cells are tuned to orientation and ocularity, BCS cell activities can be denoted as A_j^{od} where the superscript ‘o’ (ocularity) denotes ocularity (which is either ‘l’ for monocular left, ‘r’ for monocular right, or ‘b’ for binocular) and ‘d’ (degree) denotes orientation (which is either 45° or 135°).

A.4. Corticogeniculate feedback pathway (Fig. 2, Pathway 2)

The adaptive weight in the feedback pathways from the j th V1 cell to the i th LGN cell is denoted by z_{ji} , and the long-term change of synaptic efficacy in this pathway is described by:

$$\frac{d}{dt} z_{ji} = \gamma_1 A_j T_i (-z_{ji} + \kappa_1 T_i). \quad (16)$$

Term $A_j T_i$ in Eq. (16) states that adaptive weight of the feedback pathway is modified only when both presynaptic (A_j) and postsynaptic cells (T_i) are active. Term $-z_{ji} + \kappa_1 T_i$ says that the weight decreases when the postsynaptic activity T_i habituates.

Since BCS cells are tuned to ocularity and orientation and LGN cells to ocularity and color, the feedback pathway between them can be labeled by a set of four superscripts; ‘o’ (ocularity), ‘d’ (degree), ‘e’ (eye), and ‘c’ (color). For example, the pathway from the binocular BCS cell (b) with 45° orientational preference (45) to the left (l) magenta (m) LGN cell can be denoted as z_{ji}^{b45lm} . In this way, each pathway can be expressed as Eq. (16) with an appropriate use of superscripts. Initial

values before self-organization were $z_{ji} = 0.0001$ for all j, i .

The feedback pathway also acts as a gating signal for LGN output signals. Hence, the LGN output signals under the influence of feedback matching and selection, r_i are described by:

$$r_i = \sum_o \sum_d \sum_j A_j^{\text{od}} z_{ji}^{\text{odec}} T_i^{\text{ec}}. \quad (17)$$

Eq. (17) states that the feedback ($A_j z_{ji}$) modulates bottom-up output signals by a top-down multiplicative gating process of the LGN activity (T_i), summed over all ocularity (o) and orientation (d) of cortical BCS cells.

According to Eq. (17), the LGN output r_i will be zero if all the feedback gating signals A_j are zero. This might seem to imply that bottom-up signals from the LGN could never activate higher processing stages, including the boundaries that activate the terms A_j , since the boundary terms A_j would have zero activity unless they were first activated by bottom-up inputs, such as r_i . A more general expression, which replaces A_j by a constant bottom-up gain plus the top-down gain A_j , would overcome this problem. The constant bottom-up gain would enable bottom-up signals r_i to activate higher processing stages. Once activated, the top-down gain would then multiplicatively enhance bottom-up processing. In the present model, the top-down terms A_j were chosen algorithmically to be constants by Eq. (15). The present formulation with terms A_j alone is thus equivalent to a formulation with A_j plus a constant bottom-up gain, with a suitable change in the numerical values of A_j , since the simulations consider only times when both bottom-up and top-down processes are already active, and focus on more slowly varying processes like habituation and learning.

The bottom-up output signals are opponently processed (Fig. 2, Pathway 3) between magenta and green cells before they activate binocular FCS cells and initiate filling-in:

$$R_i^{\text{m|g}} = \left[r_i^{\text{m|g}} - r_i^{\text{g|m}} \right]^+. \quad (18)$$

A.5. Binocular summation

Opponent processed monocular FCS activities are transmitted to the binocular summation stage by the cortical bottom-up FCS pathway (Fig. 2, Pathway 5). The net transmitted signal, y_i , to the i th binocular FCS cell is given by:

$$y_i = R_i Z_i, \quad (19)$$

where Z_i is the adaptive weight in this pathway. The monocular signals from the left and the right eyes are binocularly summated by the following membrane equation:

$$\begin{aligned} \frac{d}{dt} s_i^b = & -A_2 s_i^b + (B_2 - s_i^b) \sum_{k=1}^N C_{2ki} [f(y_k^l) + f(y_k^r)] \\ & - (s_i^b + D_2) \sum_{k=1}^N E_{2ki} [g(y_k^l) + g(y_k^r)], \end{aligned} \quad (20)$$

where excitatory (C_{2ki}) and inhibitory (E_{2ki}) kernels are defined in the same manner as in Eqs. (9) and (10). Excitatory and inhibitory signal functions $f(x)$ and $g(x)$, respectively, are defined as:

$$f(x) = \frac{[x - \Gamma]^+2}{\alpha^2 + [x - \Gamma]^+2} \quad (21)$$

and

$$g(x) = \frac{[x - \Gamma]^+}{\alpha + [x - \Gamma]^+}, \quad (22)$$

where Γ and α are constants. In the simulations, Eq. (20) for the activity s_i^b of the i th binocular FCS cell is solved at equilibrium. The output signals from the binocular FCS are half-wave rectified:

$$S_i^b = [s_i^b]^+. \quad (23)$$

A.6. Binocular transmitter habituation

As in Eqs. (13) and (14), the transmitter levels at the binocular summation stage, t_i^b , are described by the equation:

$$\frac{d}{dt} t_i^b = \eta_2 [L_2 - (1 + \mu_2 S_i^b) t_i^b]. \quad (24)$$

Binocular transmitter habituation does not play a critical role in the model explanation of the ME, but is nevertheless incorporated in the model in order to maintain symmetry between properties of monocular and binocular FCS cells.

Transmitter-gated output obeys:

$$T_i^b = S_i^b t_i^b. \quad (25)$$

Transmitter-gated outputs are then opponently processed between magenta and green cells:

$$O_i^{b,(m|g)} = [T_i^{b,(m|g)} - T_i^{b,(g|m)}]^+. \quad (26)$$

A.7. Cortical bottom-up FCS pathway (Fig. 2, Pathway 5)

The adaptive weight in the cortical bottom-up FCS pathways from the i th monocular cortical FCS cell (R_i) to the i th binocular cortical FCS cell (O_i^b) is denoted by Z_i , and the long-term change of synaptic efficacy in this pathway is described by:

$$\frac{d}{dt} Z_i = \gamma_2 R_i O_i^b (-Z_i + \kappa_2 O_i^b), \quad (27)$$

where γ_2 is a learning rate constant, and κ_2 is a constant which determines the asymptotic value of the weight. The cortical bottom-up FCS learning described by Eq. (27) is of the same form as the corticogeniculate feedback learning described previously by Eq. (16). This learning helps to binocularly align monocular featural signals that correspond to the same object features. Since the cortical bottom-up FCS pathways connect monocular-color surfaces with binocular-color surfaces, a superscript is needed to denote each specific pathway. For example, the pathway from a monocular green cell to a binocular magenta cell is denoted as Z_i^{gm} . Initial values before self-organization were $Z_i = 0.03$ for all i .

A.8. Binocular FIDO and binocular boundary

Binocularly summated featural properties, such as color, generate a visible surface representation at the final level of the FCS, which is called Binocular FIDO. The binocular FIDO (Fig. 2, Stage VI) contains an array of intimately connected cells such that neighboring cells can rapidly spread activities between each other's compartment membranes via a process of diffusion.

The diffusive spreading, or filling-in, of activation in the binocular FIDO is restricted to the compartments that are formed by binocular boundaries, which act as barriers to filling-in. The diffusion coefficients that restrict the magnitude of cross-influence of location i with location k decrease as the binocular boundary signals B_{ji} and B_{jk} increase:

$$P_{ki} = \frac{\delta}{\beta + v \sum_o \sum_d \sum_j A_j^{\text{od}} (B_{jk}^{\text{od}} + B_{ji}^{\text{od}})}, \quad (28)$$

where δ , β , v are constants which determine the magnitude of the diffusion coefficients. Binocular boundary learning is described by:

$$\frac{d}{dt} B_{ji} = \gamma_3 A_j O_i^b (-B_{ji} + \kappa_3 O_i^b), \quad (29)$$

where γ_3 is a learning rate constant, κ_3 is a constant which determines the asymptotic value of the weight, and O_i^b is computed by sharpening binocular FCS activity O_i^b by raising it to the n th power and normalizing it:

$$o_i^b = \left[\frac{(O_i^b)^n}{[\omega^n + \sum_{k=1}^N (C_{3ki} O_k^b)^n]} - \Omega \right]^+, \quad (30)$$

where ω and Ω are constants, and the kernel C_{3ki} is defined in the same manner as in Eqs. (9) and (10). The operation in Eq. (30) sharpens spatial patterns in the FCS so that spatially localized boundary structures corresponding to the FCS patterns are formed, while ensuring analog-sensitivity of the boundary values

(i.e., large amplitudes of FCS signals result in large amplitudes of boundary signals). The BCS boundary strengths initially start out small and equal ($B_{ji} = 0.00001$ for all j, i) and then self-organize for 50 iterations of numerical integrations, as described previously.

Each activity x_i at position i of the binocular FIDO uses a nonlinear diffusion equation to fill-in surface color:

$$\frac{d}{dt}x_i = -x_i + \sum_{k \in N_i} (x_k - x_i)P_{ki} + O_i^b. \quad (31)$$

The adaptively aligned boundaries in Eq. (29) determine the permeabilities P_{ki} , which are defined by Eq. (28), and the set N_i of locations contains only the nearest neighbors of i :

$$N_i = (i - 1), (i + 1). \quad (32)$$

According to Eq. (31), each potential x_i is activated by O_i^b and thereupon engages in passive decay (term $-x_i$) and diffusive filling-in with its two nearest neighbors to the degree permitted by the diffusion coefficient P_{ki} . Opponent processing (Fig. 2, Pathway 6) of the binocular FIDO activities gives the final perceptual activity (Fig. 2, Stage VI):

$$X_i^{\text{m|g}} = \left[x_i^{\text{m|g}} - x_i^{\text{g|m}} \right]^+. \quad (33)$$

A.9. Parameters

In all simulations, the following parameter values are used.

A.9.1. Retina and LGN cells

$$N = 300, \quad \rho = 0.5, \quad A_1 = 1.0, \quad B_1 = 9.0, \quad C_1 = 4.0, \\ D_1 = 5.0, \quad E_1 = 0.4, \quad \theta_1 = 1.0, \quad \lambda_1 = 8.0.$$

A.9.2. Monocular transmitter habituation

$$\eta_1 = 0.5, \quad L_1 = 1.0, \quad \mu_1 \text{ for chromatic cell} = 1.0, \\ \mu_1 \text{ for achromatic cell} = 0.05.$$

A.9.3. BCS cells

$$B_B = 0.30, \quad M_M = 0.44, \quad B_M = 0.23, \quad M_B = 0.21.$$

A.9.4. Corticogeniculate feedback pathway

$$\gamma_1 = 0.1, \quad \kappa_1 = 1.0.$$

A.9.5. Binocular summation

$$A_2 = 10.0, \quad B_2 = 5.0, \quad C_2 = 4.0, \quad D_2 = 1.0, \quad E_2 = 0.4, \\ \theta_2 = 1.0, \quad \lambda_2 = 8.0, \quad \alpha = 3.0, \quad \Gamma = 0.0.$$

A.9.6. Binocular transmitter habituation

$$\eta_2 = 0.1, \quad L_1 = 1.0, \quad \mu_2 = 0.1.$$

A.9.7. Cortical bottom-up FCS pathway

$\kappa_2 = 0.5$, γ_2 for same color association = 0.2, γ_2 for achromatic-to-chromatic association = 0.002, γ_2 for different color association = 0.0005.

A.9.8. Binocular FIDO and binocular boundary

$$\delta = 1000.0, \quad \beta = 0.01, \quad v = 30.0, \quad \gamma_3 = 1.0, \quad \kappa_3 = 10.0, \\ \omega = 0.70, \quad C_3 = 1.0, \quad \theta_3 = 20.0, \quad n = 50.0, \quad \Omega = 0.24.$$

References

- Abbott, L. F., Varela, J. A., Sen, K., & Nelson, S. B. (1997). Synaptic depression and cortical gain control. *Science*, 275, 220–223.
- Allan, L. G., & Siegel, S. (1997). Contingent color aftereffects: reassessing old conclusions. *Perception and Psychophysics*, 59(1), 129–141.
- Baloch, A. A., Grossberg, S., Mingolla, E., & Nogueira, C. A. (1999). Neural model of first-order and second-order motion perception and magnocellular dynamics. *Journal of the Optical Society of America A*, 16(5), 953–978.
- Bedford, F. L. (1993). Keeping perception accurate. *Trends in Cognitive Sciences*, 3(1), 4–11.
- Bedford, F. L. (1995). Constraints on perceptual learning: objects and dimensions. *Cognition*, 54, 253–297.
- Bedford, F. L. (1997). Are long-term changes to perception explained by Pavlovian associations or perceptual learning theory? *Cognition*, 64, 223–230.
- Broerse, J., & O'Shea, R. P. (1995). Local and global factors in spatially-contingent coloured aftereffects. *Vision Research*, 35(2), 207–226.
- Broerse, J., Vladusich, T., & O'Shea, R. (1999). Colour at edges and colour spreading in McCollough effects. *Vision Research*, 39, 1305–1320.
- Carpenter, G. A., & Grossberg, S. (1981). Adaptation and transmitter gating in vertebrate photoreceptors. *Journal of Theoretical Neurobiology*, 1, 1–42 (Reprinted in: Grossberg, S. (1987). The adaptive brain. II. Vision, speech, language, and motor control. Amsterdam: North-Holland).
- Cohn, T. E., & Lasley, D. J. (1986). Visual sensitivity. *Annual Reviews Psychology*, 37, 495–521.
- Dodwell, P. C., & Humphrey, G. K. (1990). A functional theory of the McCollough effect. *Psychological Review*, 97(1), 78–89.
- Dresp, B., & Grossberg, S. (1997). Contour integration across polarities and spatial gaps: from local contrast filtering to global grouping. *Vision Research*, 37(7), 913–924.
- Dresp, B., & Grossberg, S. (1999). Spatial facilitation by color and luminance edges: boundary, surface, and attentional factors. *Vision Research*, 39, 3431–3443.
- Elder, J. H., & Zucker, S. W. (1998). Evidence for boundary-specific grouping. *Vision Research*, 328, 143–152.
- Francis, G., & Grossberg, S. (1996). Cortical dynamics of boundary segmentation and reset: persistence, afterimages, and residual traces. *Perception*, 25, 543–567.
- Francis, G., Grossberg, S., & Mingolla, E. (1994). Cortical dynamics of feature binding and reset: control of visual persistence. *Vision Research*, 34(8), 1089–1104.

- Gove, A., Grossberg, S., & Mingolla, E. (1995). Brightness preception, illusory contours, and corticogeniculate feedback. *Visual Neuroscience*, *12*, 1027–1052.
- Grieve, K. L., & Sillito, A. M. (1995). Differential properties of cells in the feline primary visual cortex providing the corticofugal feedback to the lateral geniculate nucleus and visual claustrum. *The Journal of Neuroscience*, *15*(7), 4868–4874.
- Grossberg, S. (1968). Some physiological and biochemical consequences of psychological postulates. *Proceedings of the National Academy of Sciences*, *60*, 758–765.
- Grossberg, S. (1969). On the production and release of chemical transmitters and related topics in cellular control. *Journal of Theoretical Biology*, *22*, 325–364.
- Grossberg, S. (1973). Contour enhancement, short-term memory and constancies in reverberating neural networks. *Studies in Applied Mathematics*, *52*, 217–257.
- Grossberg, S. (1980). How does a brain build a cognitive code? *Psychological Review*, *87*, 1–51.
- Grossberg, S. (1983). The quantized geometry of visual space: the coherent computation of depth, form, and lightness. *Behavioral and Brain Sciences*, *6*, 625–657.
- Grossberg, S. (1987). Cortical dynamics of three-dimensional form, color, and brightness perception. II. Binocular theory. *Perception and Psychophysics*, *41*(2), 117–158.
- Grossberg, S. (1994). 3-D vision and figure-ground separation by visual cortex. *Perception and Psychophysics*, *55*(1), 48–120.
- Grossberg, S. (1997). Cortical dynamics of three-dimensional figure-ground perception of two-dimensional pictures. *Psychological Review*, *104*(3), 618–658.
- Grossberg, S., & Kelly, F. (1999). Neural dynamics of binocular brightness perception. *Vision Research*, *39*(22), 3796–3816.
- Grossberg, S., & McLoughlin, N. P. (1997). Cortical dynamics of three-dimensional surface perception: binocular and half-occluded scenic images. *Neural Networks*, *10*(9), 1583–1605.
- Grossberg, S., Mingolla, E., & Ross, W. (1997). Visual brain and visual perception: how does the cortex do perceptual grouping? *Trends in Neurosciences*, *20*(3), 106–111.
- Grossberg, S., & Pessoa, L. (1998). Texture segregation, surface representation and figure-ground separation. *Vision Research*, *38*, 2657–2684.
- Grossberg, S., & Todorović, D. (1988). Neural dynamics of 1-D and 2-D brightness perception: a unified model of classical and recent phenomena. *Perception and Psychophysics*, *43*, 241–277.
- Grunewald, A., & Grossberg, S. (1998). Self-organization of binocular disparity tuning by reciprocal corticogeniculate interactions. *Journal of Cognitive Neuroscience*, *10*(2), 199–215.
- Harris, C. S. (1980). Insight or out of sight?: two examples of perceptual plasticity in the human adult. In C. S. Harris (Ed.), *Visual coding and adaptability*. New Jersey: Hillsdale.
- Hay, J. C., Pick, H. L., Jr., & Rosser, E. (1963). Adaptation to chromatic aberration by the human visual system. *Science*, *141*, 167–169.
- Held, R. (1980). The rediscovery of adaptability in the visual system: effects of extrinsic and intrinsic chromatic dispersion. In C. S. Harris (Ed.), *Visual coding and adaptability*. New Jersey: Hillsdale.
- Hohmann, A., & von der Malsburg, C. (1978). McCollough effect and eye optics. *Perception*, *7*, 551–555.
- Hubel, D. H., & Wiesel, T. N. (1962). Receptive fields, binocular interaction and functional architecture in the cat's visual cortex. *Journal of Neurophysiology*, *160*, 106–154.
- Jenkins, B., & Ross, J. (1977). McCollough effect depends upon perceived organization. *Perception*, *6*, 399–400.
- Jones, P. D., & Holding, D. H. (1975). Extremely long-term persistence of the McCollough effect. *Journal of Experimental Psychology: Human Perception and Performance*, *1*(4), 323–327.
- Kato, H., Bishop, P. O., & Orban, G. A. (1981). Binocular interaction on monocularly discharged lateral geniculate and striate neurons in the cat. *Journal of Neurophysiology*, *46*(5), 932–951.
- Kelly, F., & Grossberg, S. (2000). Neural dynamics of 3-D surface perception: figure-ground separation and lightness perception. *Perception and Psychophysics*, *62*(8), 1596–1618.
- Kohler, I. (1962). Experiments with goggles. *Scientific American*, *206*, 62–72.
- Lamme, V. A., Rodriguez-Rodriguez, V., & Spekreijse, H. (1999). Separate processing dynamics for texture elements, boundaries and surfaces in primary visual cortex of the macaque monkey. *Cerebral Cortex*, *9*, 406–413.
- Lehmkuhle, S. M., & Fox, R. (1976). On measuring interocular transfer. *Vision Research*, *16*, 428–430.
- MacKay, D. M., & MacKay, V. (1973). Orientation-sensitive after-effects of dichoptically presented colour and form. *Nature*, *242*, 477–479.
- MacKay, D. M., & MacKay, V. (1975). What causes decay of pattern-contingent chromatic aftereffects? *Vision Research*, *15*, 462–464.
- McCollough, C. (1965). Color adaptation of edge-detectors in the human visual system. *Science*, *149*, 1115–1116.
- McLoughlin, N. P. (1995). Neural network models of 3-D surface perception: Da Vinci stereopsis and the McCollough effect. Ph.D. Thesis, Boston University.
- Meyer, G. E., & Dougherty, T. (1987). Effects of flicker-induced depth on chromatic subjective contours. *Journal of Experimental Psychology: Human Perception and Performance*, *13*(3), 353–360.
- Meyer, G. E., & Phillips, D. (1980). Faces, vases, subjective contours, and the McCollough effect. *Perception*, *9*, 603–606.
- Michael, C. R. (1978). Color vision mechanisms in monkey striate cortex: simple cells with dual opponent-color receptive fields. *Journal of Neurophysiology*, *41*(5), 1233–1249.
- Murch, G. M. (1976). Classical conditioning of the McCollough effect: temporal parameters. *Vision Research*, *16*, 615–619.
- Murch, G. M., & Hirsch, J. (1972). The McCollough effect created by complementary afterimages. *American Journal of Psychology*, *85*(2), 241–247.
- Murphy, P. C., Duckett, S. G., & Sillito, A. M. (1999). Feedback connection to the lateral geniculate nucleus and cortical response properties. *Science*, *286*, 1552–1554.
- Ögmen, H., & Gagné, S. (1990). Neural models of SUSTAINED and ON-OFF units of insect lamina. *Biological Cybernetics*, *63*(1), 51–60.
- Pettigrew, J. D., Nikara, T., & Bishop, P. O. (1968). Binocular interaction on single units in cat striate cortex: simultaneous stimulation by single moving slit with receptive fields in correspondence. *Experimental Brain Research*, *6*, 391–410.
- Przybylski, A. W., Gaska, J. P., Foote, W., & Pollen, D. A. (2000). Striate cortex increases contrast gain of macaque LGN neurons. *Visual Neuroscience*, *17*, 485–494.
- Riggs, L. A., White, K. D., & Eimas, P. D. (1974). Establishment and decay of orientation-contingent aftereffects of color. *Perception and Psychophysics*, *16*(3), 535–542.
- Rogers-Ramachandran, D. C., & Ramachandran, V. S. (1998). Psychophysical evidence for boundary and surface systems in human vision. *Vision Research*, *38*, 71–77.
- Rose, D., Blake, R., & Halpern, D. L. (1989). The relationship between binocular summation, fusion, stereopsis, and allelotropia. In J. J. Kulikowski, C. M. Dickinson, & I. J. Murray (Eds.), *Seeing contour and colour* (pp. 317–323). Oxford: Pergamon.
- Savoy, R. L. (1984). “Extinction” of the McCollough effect does not transfer interocularly. *Perception and Psychophysics*, *36*(6), 571–576.
- Savoy, R. L. (1987). Contingent aftereffects and isoluminance: psychophysical evidence for separation of color, orientation, and motion. *Computer Vision, Graphics, and Image Processing*, *37*, 3–19.

- Sengpiel, F., Blakemore, C., & Harrad, R. (1995). Interocular suppression in the primary visual cortex: a possible neural basis of binocular rivalry. *Vision Research*, 35(2), 179–195.
- Shute, C. C. D. (1979). *The McCollough effect: an indicator of central neurotransmitter activity*. Cambridge: Cambridge University Press.
- Sillito, A. M., Jones, H. E., Gerstein, G. L., & West, D. C. (1994). Feature-linked synchronization of thalamic relay cell firing induced by feedback from the visual cortex. *Nature*, 369(9), 479–482.
- Skowbo, D., Gentry, T., Timney, B., & Morant, R. (1974). The McCollough effects: Influence of several kinds of visual stimulation on decay rate. *Perception and Psychophysics*, 16, 47–49.
- Skowbo, D., & White, K. (1983). McCollough effect acquisition depends on duration of exposure to inducing stimuli, not number of stimulus presentation. *Perception and Psychophysics*, 34, 549–551.
- Stromeyer, C. F. (1969). Further studies of the McCollough effect. *Perception and Psychophysics*, 6(2), 105–110.
- Stromeyer, C. F., & Dawson, B. M. (1978). Form-colour aftereffects: selectivity to local luminance contrast. *Perception*, 7, 407–415.
- Uhlark, J., Pringle, R., & Brigell, M. (1977). Color aftereffects contingent on perceptual organization. *Perception and Psychophysics*, 22(5), 506–510.
- Vidyasagar, T. R. (1976). Orientation specific colour adaptation at a binocular site. *Nature*, 261, 39–40.
- von Tschermak-Seysenegg, A. (1952). *Introduction to physiological optics (P. Boeder, Trans.)*. Springfield, IL: Thomas.
- Warren, R. M. (1985). Criterion shift rule and perceptual homeostasis. *Psychological Review*, 92(4), 574–584.
- Watanabe, T. (1995). Orientation and color processing for partially occluded objects. *Vision Research*, 35(5), 647–655.
- Watanabe, T., Zimmerman, G. L., & Cavanagh, P. (1992). Orientation-contingent color aftereffects mediated by subjective transparent structures. *Perception and Psychophysics*, 52(2), 161–166.
- Werner, H. (1937). Dynamics in binocular depth perception. *Psychological Monographs*, 48, 218, 1–127.
- White, K. D., Petry, H. M., Riggs, L. A., & Miller, J. (1978). Binocular interactions during establishment of McCollough effects. *Vision Research*, 18, 1201–1215.